The *fruitless* Gene Is Required for the Proper Formation of Axonal Tracts in the Embryonic Central Nervous System of Drosophila

Ho-Juhn Song,*[,1] Jean-Christophe Billeter,[†,2] Enrique Reynaud,[‡,3] Troy Carlo,[†] Eric P. Spana,[§,4] Norbert Perrimon,[§] Stephen F. Goodwin,[†,2] Bruce S. Baker[‡] and Barbara J. Taylor*[,5]

**Department of Zoology, Oregon State University, Corvallis, Oregon 97331-2914, [†]Department of Biology, Brandeis University, Waltham, Massachusetts 02454-9110, [‡]Department of Biological Sciences, Stanford University, Stanford, California 94305-5020 and [§]Department of Genetics, Harvard Medical School, Boston, Massachusetts 02115*

Manuscript received January 14, 2002
Accepted for publication September 19, 2002

ABSTRACT

The *fruitless* (*fru*) gene in *Drosophila melanogaster* is a multifunctional gene that has sex-specific functions in the regulation of male sexual behavior and sex-nonspecific functions affecting adult viability and external morphology. While much attention has focused on *fru*'s sex-specific roles, less is known about its sex-nonspecific functions. We have examined *fru*'s sex-nonspecific role in embryonic neural development. *fru* transcripts from sex-nonspecific promoters are expressed beginning at the earliest stages of neurogenesis, and Fru proteins are present in both neurons and glia. In embryos that lack most or all *fru* function, FasII- and BP102-positive axons have defasciculation defects and grow along abnormal pathways in the CNS. These defects in axonal projections in *fru* mutants were rescued by the expression of specific *UAS-fru* transgenes under the control of a pan-neuronal *scabrous-GAL4* driver. Our results suggest that one of *fru*'s sex-nonspecific roles is to regulate the pathfinding ability of axons in the embryonic CNS.

THE *fruitless* (*fru*) gene has a prominent role in developing the potential for male sexual behavior as well as adult viability and normal external morphology (Ito *et al.* 1996; Ryner *et al.* 1996; Goodwin *et al.* 2000; Usui-Aoki *et al.* 2000; Anand *et al.* 2001; Lee and Hall 2001; Lee *et al.* 2001). *fru*'s functional complexity is reflected in the structural complexity of the locus. The *fru* gene encodes a large set of sex-specific and sex-nonspecific transcripts generated by differential promoter usage and alternative splicing at the 5′ and 3′ ends (Ito *et al.* 1996; Ryner *et al.* 1996; Goodwin *et al.* 2000; Usui-Aoki *et al.* 2000). *fru* transcripts from four different promoters, P1, P2, P3, and P4, encode closely related BTB/POZ (*B*road complex, *T*ramtrack, and *B*ric-a-brac/*Po*xvirus and *Z*inc finger)-Zn finger (ZnF) proteins, which likely act as transcription factors (Ito *et al.* 1996; Ryner *et al.* 1996; Goodwin *et al.* 2000; Lee *et al.* 2000; Usui-Aoki *et al.* 2000; Anand *et al.* 2001).

The male-specific behavioral functions of *fru* depend on transcripts produced from the P1 promoter that are sex-specifically spliced (Ito *et al.* 1996; Ryner *et al.* 1996; Goodwin *et al.* 2000; Usui-Aoki *et al.* 2000; Anand *et al.* 2001). In males a default 5′ acceptor splice site is used, whereas in females, the Transformer (Tra) and Transformer-2 (Tra-2) proteins direct splicing to a second downstream acceptor site (Ryner *et al.* 1996; Heinrichs *et al.* 1998; Usui-Aoki *et al.* 2000). In both sexes, alternative splicing at the 3′ end leads to the generation of three types of P1 transcripts, each with a different pair of ZnF domains (Goodwin *et al.* 2000; Usui-Aoki *et al.* 2000). A consequence of the sex-specific splicing of P1 primary transcripts is the generation of a set of P1 transcripts in males, which upon translation produce a family of proteins with an amino-terminal extension preceding the BTB/POZ domain and a set of P1 transcripts in females, which are not translated (Ito *et al.* 1996; Ryner *et al.* 1996; Goodwin *et al.* 2000; Lee *et al.* 2000; Usui-Aoki *et al.* 2000). The male-specific P1 transcripts are translated into male-specific Fru proteins (Fru^M), which are expressed in nearly 2000 neurons in the pupal and adult central nervous system (CNS) and play an important role in male sexual behavior and in the formation of a male-specific abdominal muscle known as the muscle of Lawrence (Ito *et al.* 1996; Ryner *et al.* 1996; Goodwin *et al.* 2000; Lee *et al.* 2000; Usui-Aoki *et al.* 2000; Anand *et al.* 2001). Recently, it has been shown that the Fru^M proteins are required for the presence of the serotonin neurotransmitter in a set of abdominal neurons that innervate the masculine internal genitalia and mediate aspects of male fertility (Lee and Hall 2001; Lee *et al.* 2001).

[1]*Present address:* Functional Genomics Department, Novartis Pharmaceuticals, Summit, NJ 07901.

[2]*Present address:* Division of Molecular Genetics, University of Glasgow, Glasgow G11 6NU, United Kingdom.

[3]*Present address:* Departamento de Genética del Desarrollo, Instituto de Biotecnología, Universidad Nacional Autónoma de México (UNAM), Cuernavaca Morelos 62250, Mexico.

[4]*Present address:* Syngenta Biotechnology Inc., Research Triangle Park, NC 27709-2257.

[5]*Corresponding author:* Department of Zoology, 3029 Cordley Hall, Oregon State University, Corvallis, OR 97331-2914.
E-mail: taylorb@bcc.orst.edu

The products of the P2, P3, and P4 *fru* promoters differ from those of the P1 promoter in their spatial patterns of expression, their protein coding sequences, and their functions (Ryner *et al.* 1996; Goodwin *et al.* 2000; Anand *et al.* 2001). Transcripts from the P2, P3, and P4 promoters encode a small amino-terminal extension of a few amino acids preceding the common BTB/POZ domain compared to the 101 amino-terminal motif found in the P1-derived male-specific proteins (S. F. Goodwin, L. C. Ryner, T. Carlo, M. Foss, J. C. Hall, B. J. Taylor and B. S. Baker, unpublished results). *In situ* hybridization using a probe from the common coding region of *fru*, which detects all or most of the known *fru* transcripts, shows that *fru* transcripts from non-P1 promoters are ubiquitously expressed in the adult CNS and in particular subsets of nonneuronal tissues during larval and pupal development of both adult male and female flies (Ryner *et al.* 1996; Goodwin *et al.* 2000; Lee *et al.* 2000). Anti-Fru antibodies, which recognize the common region of Fru proteins, confirm that these *fru* RNAs are translated in both sexes in the CNS and nonneuronal tissues (Lee *et al.* 2000). Genetic analysis of *fru* mutants shows that mutants lacking the P3 and/or P4 transcript classes die at the pupal stage, suggesting that the expression of a subset of *fru* transcripts is essential for adult viability (Ryner *et al.* 1996; Anand *et al.* 2001). In some *fru* mutant genotypes, adult escapers show a variety of defective external phenotypes, indicating that these transcripts likely have some function in the development of these adult structures (Anand *et al.* 2001).

To gain a better understanding of the role of *fru*'s P2, P3, and P4 transcripts in development, we determined the expression pattern of *fru* RNAs and proteins in the embryonic CNS. In this article, we show that *fru* RNAs and proteins are produced in a dynamic pattern during embryogenesis and are widely expressed in the developing embryonic CNS. Neuronal precursors as well as neurons and glial cells express Fru proteins. The embryonic CNS is an important model system for defining how specific genes govern neuronal identity and the process of axonal pathfinding necessary for the formation of proper neuronal connections (reviewed in Goodman and Doe 1993; Goodman 1996; Tear 1999). The main axonal tracts in the ventral nerve cord of the fruit fly embryonic CNS consist of two bilaterally symmetrical longitudinal connectives with a pair of commissures, anterior and posterior, that cross the midline in each segment (Goodman and Doe 1993). The proper formation of this longitudinal and commissural axon scaffold is complex and involves the directed growth of axonal processes from interneurons and motoneurons in specific fascicles within the CNS (*e.g.*, reviewed in Tear 1999 and Rusch and Van Vactor 2000). Diffusible molecules secreted from cells along the midline are one of the mechanisms involved in attracting or repulsing specific axons (Guthrie 1999; reviewed in Tear 1999; Brose and Tessier-Lavigne 2000). Axons, as they grow through the CNS, selectively fasciculate and defasciculate to find their appropriate synaptic targets (Tear 1999; Rusch and Van Vactor 2000).

Analyses of *fru* mutants, in which specific subsets of transcripts are disrupted or in which no *fru* transcripts are made, revealed that Fasciclin II (FasII)-positive axons had abnormal trajectories, as did axons producing other longitudinal and commissural tracts in the CNS. Our findings suggest that *fru* transcripts are needed in the embryonic CNS for the formation of the wild-type pattern of axonal tracts. The defects in the FasII-positive and BP102-positive axonal tracts found in *fru* mutants were rescued by the expression of specific *fru* isoforms under the control of the pan-neuronal *sca-GAL4* driver, which has a pattern of expression similar to that of Fru proteins. In contrast, these mutant phenotypes were not rescued by *fru* transgene expression driven by the *elav-GAL4* driver, which is expressed exclusively in postmitotic neurons. The neurons that pioneer the FasII fascicles express markers appropriate to their wild-type identity in *fru* mutants. Our analysis suggests that *fru*'s primary function during neurogenesis is the regulation of fasciculation and defasciculation processes involved in the growth of neuronal axons along their wild-type pathway through the CNS.

MATERIALS AND METHODS

Fly stocks and crosses: Canton-S flies were used as the wild-type genotype. The following *fru* mutant alleles were used: fru^{3}; fru^{4}; fru^{sat}; *In(3R)fru*^{1} (fru^{1}); *Df(3R)Cha*^{M5} (Cha^{M5}); *Df(3R)fru*^{w24} (fru^{w24}); *In(3R) fru*^{w27} (fru^{w27}); *Df(3R)fru*^{sat15} (fru^{sat15}); *Df(3R)fru*$^{4-40}$ (fru^{4-40}); *In(3R)fru*^{w12} (fru^{w12}); *Df(3R)P14* (*P14*) (Castrillon *et al.* 1993; Ito *et al.* 1996; Ryner *et al.* 1996; Anand *et al.* 2001). *fru* mutant alleles were maintained over either *TM6B, Tb, Hu* or *TM3, Sb, P[ftz-lacZ]*. To label midline glial cells in *fru* mutants (see below), the *P* element in the enhancer-trap line *AA142* (Scholz *et al.* 1997; Bloomington Stock Center) was recombined onto the fru^{sat15} and fru^{AJ96u3} chromosomes. Fly stocks were maintained at room temperature on an agar, sucrose, cornmeal, and yeast medium supplemented with 0.1% nipagin (p-hydroxybenzoic acid methyl ester; Sigma, St. Louis) for mold inhibition.

A deficiency, *Df(3L)XDI98* (65A02-65E1), was used to examine the phenotypes associated with the non-*fru* inversion breakpoint, at 65C-D, of the fru^{w12} chromosome. fru^{w12}/*Df(3L)XDI98* mutants were fully viable, fertile, and morphologically normal adults (n = 10 male; n = 10 female). Deficiency heterozygous males did not show courtship chaining behaviors, a typical *fru* mutant phenotype (n = 20, 10 males each group). Due to the similarity of phenotypes, a *spread* mutant allele ($sprd^{05284}$; Spradling *et al.* 1999; Bloomington Stock Center) was used in complementation tests with various *fru* mutations. There were no adult $sprd^{05284}/fru^{w24}$ survivors, indicating that large *fru* deficiencies uncover the *sprd* locus (0/36 control siblings). However, $sprd^{05284}$ *trans*-heterozygotes with other *fru* alleles were fully viable with a normal wing phenotype ($sprd^{05284}/fru^{4-40}$, n = 61; $sprd^{05284}/fru^{w12}$, n = 30; $sprd^{05284}/fru^{AJ96u3}$, n = 24) and did not form male-male courtship chains ($sprd^{05284}/fru^{4-40}$, n = 20; $sprd^{05284}/fru^{w12}$, n = 8; $sprd^{05284}/fru^{AJ96u3}$, n = 9).

Generation and molecular characterization of the fru^{AJ96u3} deficiency: The $AJ96w^+$ *P* element (Spana and Doe 1996) was mapped by isolating flanking genomic sequences using inverse PCR followed by sequencing (Yeo *et al.* 1995). These query sequences were used for BLAST homology searches against the Drosophila genome and mapped to genomic sequences that include the *fru* locus (accession no. AE003722; FlyBase 1999). To create new *fru* mutations, excisions of the $AJ96w^+$ *P* element were induced by standard techniques (Robertson *et al.* 1988). One lethal excision out of 56 w^- revertant lines was recovered. The molecular limits of the fru^{AJ96u3} deficiency were determined by a combination of Southern blot analysis and genomic PCR using oligo primers obtained from plasmid subclones from across the *fru* region and flanking sequences (data not shown). The exact molecular locations of the deficiency breakpoints were determined by using oligo primers, flanking these sequences, to PCR amplify fragments that contain sequences around the breakpoints. These PCR fragments were sequenced and compared to the published sequences for this region.

Lethal phase, phenotypic, fertility, and behavioral analysis of fru^{AJ96u3} mutant animals: To characterize the fru^{AJ96u3} mutation, *trans*-heterozygotes between fru^{AJ96u3} and other *fru* alleles were examined. In those crosses in which adult *fru trans*-heterozygotes did not survive, the pupal stage at which the *fru* mutant combination died was determined from aged collections of white prepupae and by staging based on Bainbridge and Bownes (1981). For genotypes that reached late stages of pupal development, the pupal case was dissected to allow the animals to emerge.

For sterility tests, virgin males were collected a few hours after eclosion and housed as groups of 8–10 males in food vials. After 4 days, individual males were mated with 2 or 3 Canton-S virgin females and the vials were examined after 7 days for the presence of larvae and/or pupae. To determine whether males would form courtship chains (Villella *et al.* 1997), males were collected after eclosion and aged alone for 3–4 days. Eight males of the same genotype were then put together in a food vial and observed in the late afternoon or early evening for the presence of male courtship chains with >3 males courting during a 1-hr period over 3–4 days.

Embryonic immunohistochemistry: Timed embryo collections were staged by morphological criteria (Campos-Ortega and Hartenstein 1997) and prepared for immunohistochemistry according to Patel (1994). The following primary antibodies were used (except where noted, these antibodies were a gift from N. Patel) to label neurons and glial cells: anti-Fasciclin II (1D4, 1:5; Grenningloh *et al.* 1991), mab22C10 (1:200; Fujita *et al.* 1982), anti-Elav (9F8, 1:30; O'Neill *et al.* 1994), mabBP102 (1:20; Seeger *et al.* 1993), anti-Repo (1:100; a gift of A. Travers; Halter *et al.* 1995), anti-Engrailed/Invected (4D9, 1:10; Patel *et al.* 1989), and anti-Odd-skipped (1:200; a gift from J. Skeath; Spana *et al.* 1995). To label *fru*-positive cells, rat anti-Fru^{COM} (1:500; Lee *et al.* 2000), rat anti-$Fru^{BTB'}$ (1:500; this study, see below), rat anti-$Fru^{A'}$ (1:500; this study), and rat anti-$Fru^{C'}$ (1:500; this study) were used. In all experiments, embryos were labeled with anti β-galactosidase antibodies (1:10,000; Cappel, Durham, NC) to distinguish *fru* mutant embryos (β-galactosidase negative) from control sibling embryos (β-galactosidase positive).

For detection of primary antibodies, we used secondary antibodies, which were directly conjugated with horseradish peroxidase (Jackson ImmunoResearch Laboratories, West Grove, PA), with alkaline phosphatase (AP; Jackson ImmunoResearch), or with the fluorochromes Alexa-594, Alexa-488, or Alexa-395 (Molecular Probes, Eugene, OR). For anti-*Repo* labeling, a biotinylated secondary antibody was used followed by incubation with the ABC reagent (Vector Laboratories, Burlingame, CA). For some double-label experiments, colorimetric visualization of diaminobenzidine (Sigma) was nickel enhanced (Patel 1994). Enzymatic processing of alkaline phosphatase used NBT/X-phosphatase (Boehringer Mannheim, Indianapolis) in AP reaction buffer (0.1 M NaCl, 0.1 M Tris-HCl, pH 9.5, 0.05 M $MgCl_2$, 0.1% Tween 20; Patel 1994). To improve the signal obtained from the anti-Fru antibodies, we used the tyramide-based signal amplification kit (New England Nuclear, Boston) prior to staining for AP.

Labeled whole-mount and filleted embryos were viewed and photographed with a Sony DKC-5000 digital camera under differential interference contrast optics, using an Olympus Vanox-TX microscope. For certain double- or triple-labeling experiments, fluorescently labeled embryos were viewed on a TCS-Leica confocal microscope. Composite images were assembled in Adobe Photoshop 5.0.

***In situ* hybridization of embryos:** Single-strand antisense and sense riboprobes for *in situ* hybridization were prepared as previously described (Ryner *et al.* 1996; Goodwin *et al.* 2000). The following antisense riboprobes were used: the common coding region probe (antisense-Com, nucleotides (nt) 2785–3612, GenBank accession no. U72492), the BTB domain region probe (nt 2075–2422, GenBank accession no. U72492), the P1-promoter-derived sex-specific probe (probe P1.S, nt 160,236–159,918, accession no. AE003722), the P2 5′ end probe (nt 121,168–121,101 plus 120,967–120,936; AE0037222.2), the P3 5′ end probe (nt 95,033–94,958, accession no. AE003722), the P4 5′ end probes (nt 61,666–61,268, accession no. AE003722), and the Zn finger motif probes A (nt 1743–2294, accession no. D84437), B (nt 37,721–37,479, accession no. AE003722), and C (nt 3872–4114, GenBank accession no. U72492).

The protocols for fixation and *in situ* hybridization were according to Broadus and Doe (1995) except that RNase treatment (1 mg/ml) was included after hybridization to minimize nonspecific binding of the riboprobe. To visualize the signal, embryos were incubated in dilute anti-digoxigenin-AP (1:2000) and reacted for AP (Broadus and Doe 1995). Embryos were mounted in 70% glycerol and viewed as either whole-mount or dissected preparations.

Generation of transformants: Six different *UAS-fru* constructs were made from *fru* cDNAs subcloned in pBluescript KS (Ryner *et al.* 1996; S. F. Goodwin, L. C. Ryner, T. Carlo, M. Foss, J. C. Hall, B. J. Taylor and B. S. Baker unpublished results). These constructs all have a minimal 5′-untranslated region (UTR) and were subcloned into a pUAST vector (Brand and Perrimon 1993; van Roessel and Brand 2000). The *UAS-fruA*, *UAS-fruB*, and *UAS-fruC* constructs all started at the same 5′ *Eco*RI site (128,354, accession no. AE003722.2) and included identical 5′-UTR, BTB, and common *fru* coding sequences but different 3′ end sequences. The *UAS-fruA* construct contains a 3-kb *Eco*RI fragment of *fru* cDNA no. 7 (L. C. Ryner, personal communication; the A 3′ end terminates at nt 40563, accession no. AE003722.2). The *UAS-fruB* construct contains a 4.5-kb *Eco*RI-*Xba*I fragment from a *fru* cDNA no. 25 (L. C. Ryner, personal communication; the B 3′ terminates at nt 36684, accession no. AE003722.2). The *UAS-fruC* construct contains a 3.6-kb *Eco*RI-*Kpn*I fragment of the female cDNA no. 1 (GenBank accession no. U72492, nt 1763–5409). The *UAS-fruMA*, *UAS-fruMB*, or *UAS-fruMC* constructs all have the same 5′ sequences, which encode the 101 male-specific amino terminus and the BTB domain derived from *fru* male cDNA nos. 5-19 (L. C. Ryner, personal communication). This cDNA was truncated at the 3′ end and subcloned into pMartini (a gift from N. Brown) as a *Sac*I-*Pvu*I fragment. The final constructs were generated via a three-way ligation into the pUAST vector. The 5′ sequences (1.2-kb *Eco*RI-*Pvu*I fragment) were ligated to a 1.948-kb *Pvu*I-*Eco*RI fragment (A 3′ end; *fru*

cDNA no. 7; L. C. Ryner, personal communication), a 1.98-kb *Pvu*I-*Hind*III fragment (B′ end; *fru* cDNA no. 25; L. C. Ryner, personal communication), or a 1.98-kb *Pvu*I-*Kpn*I (C 3′ end; nt 2824–5409, GenBank accession no. U72492). These constructs would encode Fru proteins like those from P4 transcripts and similar to those from P2 and P3 transcripts, which have N-terminal extensions of a few more amino acids than P4 Fru proteins (S. F. Goodwin, L. C. Ryner, T. Carlo, M. Foss, J. C. Hall, B. J. Taylor and B. S. Baker, unpublished results).

The pUAST vectors also contained a mini-*white* reporter gene and the final transgene constructs were introduced into the *Df(1)yw* parental strain by germline transformation as described in Rubin and Spradling (1982). Transgene constructs (300 μg/ml) were coinjected with the helper plasmid pUCHSΔ2-3 (100 μg/ml). The chromosomal location of 3–10 transformant lines was determined. If a transformant line contained two insertions on different chromosomes, the transgenes were segregated and treated as independent lines. Each *UAS-fru* construct was crossed into a fru^{W12} or fru^{sat15} mutant background and balanced over *TM3, Sb*, and *P[ftz-lacZ]*. At least two independent lines for each construct were tested and analyzed.

To express these various *UAS-fru* constructs in the CNS, lines containing *scabrous-GAL4* (*sca-GAL4*) and *embryonic lethal abnormal vision-GAL4* C155 (*elav-GAL4*; Lin and Goodman 1994; Bloomington Stock Center) transgenes were crossed into a fru^{W12} or fru^{sat15} mutant background. The *scabrous* sequences in the transgenic construct drive pan-neuronal expression of GAL4 from neuroblasts through neurons (Klaes *et al.* 1994; see below) and the *elav* sequences in this transgenic construct drive expression in postmitotic neurons (Lin and Goodman 1994). Crosses between a *GAL4* line and a *UAS-fru* line generated the *fru* mutant embryos in which one of the *fru* isoforms was expressed in the CNS and peripheral nervous system (PNS). To distinguish *fru* mutant embryos from control siblings, all embryos were labeled with anti-β-galactosidase (1:10,000; Cappel), which permitted unlabeled *fru* mutant embryos to be distinguished from labeled control siblings, expressing the *lacZ* marker.

Generation of Fru antibodies: For the glutathione S-transferase (GST) fusion constructs, coding regions for the *fru* BTB domain and alternative ZnF A and C (Figure 1) were generated by PCR. Oligonucleotide pairs containing sites for in-frame directional cloning in the pGEX-4T-1 vector (Pharmacia, Piscataway, NJ) were designed for BTB and each unique ZnF sequence. DNA was amplified from *fru* cDNA clones (primer sequences for BTB domain are BTB-1-For, GGG GGA ATT CAT GGA CCA GCA ATT CTG CTT 3′; BTB-115-Rev, GGG GGC TCG AGC TAG TTG TTA TCT GTG AGA 3′; those for A form ZnF domain are A-For, 5′ CCG GAA TTC CAG CAG CGC CCG CCA CC 3′; A-Rev, 5′ GCC GCT CGA GCG GGA TGG GCT GCA CTT GGG C; and those for C form ZnF domain are C-For, 5′ CCG GAA TTC CGC GTC AAG TGT TTT AAC ATT AAG C 3′; C-Rev, 5′ CCG CTC GAG GTT TGC TTG ATT CTT GGT TAC TTA G 3′), digested with *Eco*RI and *Xho*I enzymes, and cloned into the polylinker of the pGEX-4T-1 vector. Individual recombinant clones were validated by sequencing.

Fusion proteins were purified according to Smith (1993). These fusion proteins were SDS-PAGE purified and not proteolytically cleaved from the GST so that the whole GST-ZINC FINGER or GST-BTB peptides were used as the immunogen. These materials were injected into rats using a 77-day protocol. In brief, 750 μg of purified protein was injected into each animal with complete Freund's adjuvant, followed by three 750-μg immunizations (boosters) using incomplete Freund's adjuvant. Serum was collected by exsanguinations at the end of the protocol. Titer and specificity of the antibodies were assayed by Western blots of the recombinant protein (data not shown). Harvested polyclonal antisera against the *fru* BTB domain and the A and C forms of the ZnF domain hereafter are named as anti-$Fru^{BTB'}$, anti-$Fru^{A'}$, and anti-$Fru^{C'}$, respectively.

Statistics: The frequency of defective embryos in various *fru* mutant and wild-type embryos was analyzed statistically by one-way ANOVA (SAS program version 6.12; SAS Institute) and *post hoc* analyzed by Tukey HSD comparisons or by two-sample *t*-test (SAS program version 6.12).

RESULTS

Isolation and characterization of a new *fru* null mutation: The $AJ96w^+$ *P* element, which labels a pair of midline neurons in each segment of the embryonic CNS, was mapped molecularly to ~3 kb downstream of the 3′ end of the *fru* locus (Figure 1; materials and methods; Spana and Doe 1996). Homozygous $AJ96w^+$ males did not have a *fru* mutant phenotype as they were fertile (31/32 males, each paired with two or three virgin Canton-S females) and failed to form male-male courtship chains (six tests of 8 males each; total $n = 48$).

We mobilized this *P* element and generated a deficiency line, $Df(3R)AJ96^{U3}$ (fru^{AJ96u3}). This deletion extends from sequences within the $AJ96w^+$ *P* element to sequences between the P3 and P4 promoters, thus deleting all *fru* common coding sequences (Figure 1; see materials and methods). As the smallest available deficiency of the *fru* locus, it appears to remove *fru* and only one other putative open reading frame located between the 3′ end of the *fru* locus and the $AJ96w^+$ *P* element (29,144–27,188 bp, accession no. AE003722; FlyBase 1999). Phenotypic analysis confirmed that fru^{AJ96u3} is a *fru* null allele. fru^{AJ96u3} *trans*-heterozygotes with hypomorphic *fru* alleles were fully viable (Table 1A) but were sterile (0/18 fertile $fru^{4\text{-}40}/fru^{AJ96u3}$ males; 0/18 fertile fru^{4}/fru^{AJ96u3} males). *fru trans*-heterozygotes with strong *fru* alleles, such as fru^{w27}/fru^{AJ96u3}, survived to late pupal stages and often would emerge if dissected out of the pupal case, but had striking visible external defects, such as uninflated wings or malformed leg joints (Table 1, C and D; see also Anand *et al.* 2001). By comparison, fru^{AJ96u3} *trans*-heterozygotes with *fru* null alleles, such as fru^{sat15}, survived to early pupal stages, dying at or just after pupal ecdysis, the same lethal phase of other known *fru* nulls (Table 1B; Anand *et al.* 2001). To address the possibility that some phenotypes of these *fru* escapers might be due to loss of function in the nearby *spread* gene (*sprd*, map location 91A5-6; Spradling *et al.* 1999), we performed complementation testing with various *fru* alleles and deficiencies. Our results show that these *fru* mutations fully complement this *sprd* mutation, supporting the attribution of the lethality and visible mutant phenotypes to the loss of *fru* function (see materials and methods; Anand *et al.* 2001).

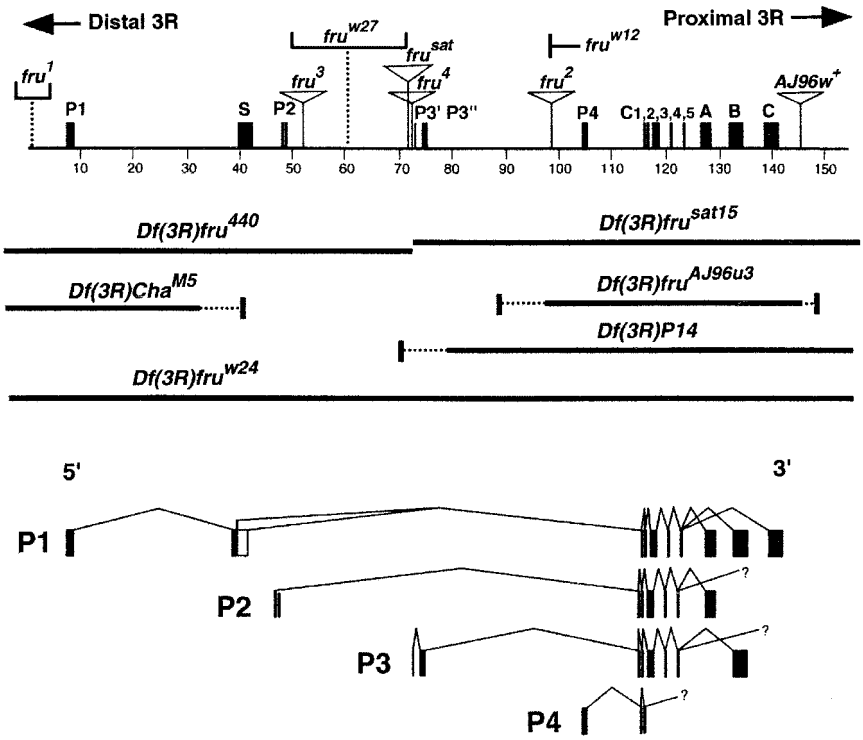

FIGURE 1.—The molecular map of the *fru* locus. The insertion sites of the *P* elements, fru^2, fru^3, fru^4, fru^{sat}, and $AJ96w^+$, are indicated by triangles (ITO *et al.* 1996; RYNER *et al.* 1996; GOODWIN *et al.* 2000; ANAND *et al.* 2001; this article). The $AJ96w^+$ *P* element is located 3 kb from the 3′ end of the *fru* locus (this article). The *fru* breakpoints of the inversion alleles fru^1 and fru^{w12} are shown on the genomic map, but the inversion allele fru^{w27} is more complex with the relevant break somewhere between P2 and P3, since no P2 transcripts are detected by reverse transcriptase-PCR (ANAND *et al.* 2001). The limits of relevant *fru* deficiencies, including the $Df(3R)fru^{AJ96u3}$ described in this article, are delineated with thick black lines to represent deleted sequences and dashed lines to represent breakpoints mapped to the relevant restriction fragment (ANAND *et al.* 2001; this article). *fru* exons are positioned on the genomic map. Four promoters (P1–P4) are distributed throughout the locus and there are three alternative 3′ ends (A, B, and C). Each 3′ end encodes a different pair of ZnF domains (GOODWIN *et al.* 2000; USUI-AOKI *et al.* 2000; S. F. GOODWIN, L. C. RYNER, T. CARLO, M. FOSS, J. C. HALL, B. J. TAYLOR and B. S. BAKER, unpublished results). The P1 promoter produces primary transcripts that are spliced in females specifically by the TRA and TRA-2 proteins binding to three repeats located in the S exon. These transcripts also contain the BTB domain and other common exons (C1–5) and are spliced alternatively to one of the three different 3′ ends (RYNER *et al.* 1996; GOODWIN *et al.* 2000; USUI-AOKI *et al.* 2000). Transcripts derived from the other three promoters, P2, P3, and P4, contain the BTB and common exons but it is not known whether these transcripts utilize all of the possible alternative 3′ ends. Therefore, the full extent of transcript complexity from these promoters is not known (RYNER *et al.* 1996; GOODWIN *et al.* 2000; USUI-AOKI *et al.* 2000; ANAND *et al.* 2001; S. F. GOODWIN, L. C. RYNER, T. CARLO, M. FOSS, J. C. HALL, B. J. TAYLOR and B. S. BAKER, unpublished results).

Temporal and spatial distribution of *fru* mRNA during embryogenesis: To determine the spatial and temporal distribution of embyonic *fru* transcripts, we performed *in situ* hybridizations with antisense-BTB and antisense-Com riboprobes, which detect most or all *fru* transcripts (RYNER *et al.* 1996; GOODWIN *et al.* 2000; LEE *et al.* 2000). We found that *fru* mRNAs are expressed in a dynamic temporal and spatial pattern from the beginning of embryogenesis until stage 16 (Figure 2; Table 2A). *fru* transcripts are uniformly distributed in very early embryos and become incorporated into segregating pole cells [stages (st) 1–5; Figure 2A]. At the start of gastrulation (st 6), heavily labeled cells are found in the ventral and cephalic furrows. In slightly older embryos (st 7–9; Figure 2B) the most prominent distribution of *fru* transcripts is found in the developing CNS within mesectodermal and ventral neuroectodermal cells. Transcripts become localized to delaminating neuroblasts (Figure 2, B and G) and after stage 10, *fru* transcripts are detected in medial but not in lateral neuroblasts (Figure 2H). Following expression in the progeny of neuroblasts, the level of *fru* expression in the CNS continues to decline until becoming undetectable at stage 16 (Table 2A; Figure 2I). Thus, *fru* transcripts are expressed throughout the development and early differentiation of the CNS but become undetectable at later stages. Cells in some non-CNS tissues, the amnioserosa and tracheal placodes, also expressed *fru* transcripts (st 9–11; Table 2A), but no *in situ* hybridization signal was detected in other tissues, such as the PNS or body wall muscles.

The *fru* locus encodes a complex set of transcripts (Figure 1; RYNER *et al.* 1996; GOODWIN *et al.* 2000; USUI-AOKI *et al.* 2000). To better understand the embryonic pattern of *fru* transcripts, we performed *in situ* hybridization with a set of 5′ end riboprobes to distinguish transcripts made from different *fru* promoters (see MATERIALS AND METHODS; RYNER *et al.* 1996; GOODWIN *et al.* 2000). We were unable to detect P1 or P2 transcripts at any embryonic stage using riboprobes specific to these transcripts (Table 2A). Thus, P1 transcripts, which encode the male-specific *fru* proteins, are not expressed in the embryo, a finding consistent with LEE *et al.* (2000). Transcripts from P3 and P4 promoters were expressed during embryogenesis in a temporal and spatial pattern that mirrored that of *fru* transcripts detected by antisense-BTB or -Com riboprobes (Table 2A). In the developing CNS, both P3- and P4-specific riboprobes labeled mesectodermal and neuroectodermal cells followed by labeling of delaminating neuroblasts (Table 2A). At slightly later stages (st 9–11), medial neuroblasts contin-

TABLE 1

Mutant phenotypes of fru^{AJ96u3} homozygotes and heterozygotes with other *fru* alleles

Genotype	No. of adult *trans*-heterozygotes/ total progeny	Genotype	No. of adult *trans*-heterozygotes/ total progeny
A. Adult viability of fru^{AJ96u3} *trans*-heterozygotes with representative *fru* alleles			
fru^{4}/fru^{AJ96u3}	99 (305)	fru^{4-40}/fru^{AJ96u3}	161 (432)
Cha^{M5}/fru^{AJ96u3}	146 (379)	fru^{w12}/fru^{AJ96u3}	0 (644)

Genotype	*N*	% brown prepupa (st P2/P3)	% bubble stage (st P4i/P4ii)	% pupal ecdysis (st P5)
B. Lethal phase of fru^{AJ96u3} *trans*-heterozygotes with *fru* null alleles				
$fru^{AJ96u3}/fru^{AJ96u3}$	72	4	96	
fru^{sat15}/fru^{AJ96u3}	50		100	
$P14/fru^{AJ96u3}$	113	40	60	
fru^{w24}/fru^{AJ96u3}	109		39	61

Genotype	*N*	% prepupal (st P2–P4)	% midpupal (st P5–P13)	% late pupal (st P14–P15ii)	% adult with dissection
C. Lethal phase of fru^{AJ96u3} *trans*-heterozygotes with strong *fru* alleles					
fru^{w12}/fru^{AJ96u3}	381	1	34	9	56
fru^{w27}/fru^{AJ96u3}	60	12	10	22	53 (3[a])

	% uneverted discs[b]		% uninflated wing		% 70°–90° wing position[c]		% defective leg joint		% duplicated bristles[d]	
Genotype	M	F	M	F	M	F	M	F	M	F
D. External phenotypes of fru^{AJ96u3} *trans*-heterozygote adult escapers										
fru^{w27}/fru^{AJ96u3} (M = 18, F = 11)	100	63	89	63	38	100	63	72	100	100

Standard crosses were made to determine the viability of various *fru* mutant *trans*-heterozygotes; in three of the crosses the *trans*-heterozygotes were fully viable since their number was within the Mendelian expectations for the cross. To determine the lethal phase during pupal development, animals were collected as white prepupae and aged until they no longer appeared to develop. The stage at which they ceased development was assessed by reference to the metamorphic stages described in Bainbridge and Bownes (1981). To simplify presentation of this table, some stages were grouped together. In some genotypes, a small number of animals, in parentheses, emerged on their own. The phenotype of adult escapers was determined for fru^{w27}/fru^{AJ96u3} animals that were dissected out of the pupal case. *N*, total number of *trans*-heterozygotes scored.

[a] The number of adult survivors that eclosed on their own.

[b] This phenotype was scored as positive if one uneverted was found per animal.

[c] Only wings that were inflated were scored for their position with respect to the body.

[d] Only the anterior scutellar and the sternopleural bristles in the thorax were obviously duplicated.

ued to express P3 and P4 transcripts, but lateral neuroblasts no longer had detectable transcripts. In stages 7–12 embryos, the *in situ* hybridization signal for P4 transcripts was less intense, suggesting that the level of P4 transcripts was lower than that of P3 transcripts in these stages. However, P3 transcript levels became undetectable in all tissues after stage 12, whereas P4 transcripts were still detectable up to stage 16 (Table 2A). In summary, the *in situ* hybridization data show that both P3 and P4 *fru* transcripts are expressed in the developing CNS and, very likely, in the same cells. Furthermore, the higher level of *fru* transcripts detected with riboprobes to *fru* common sequences in stages 9–12 CNSs is likely due to the presence of both P3 and P4 transcripts whereas the lower level of *fru* transcripts in stages 12–16 CNSs reflects the presence of only P4 transcripts.

An additional complexity in *fru* transcripts reflects alternative splicing at the 3′ end, which generates transcripts containing one of three different pairs of Zn-finger domains (Figure 1; Ryner *et al.* 1996; Goodwin *et al.* 2000; Usui-Aoki *et al.* 2000). While it is known that P1 transcript isoforms are spliced to each of the three alternative 3′ ends (Goodwin *et al.* 2000), the full complexity of the 3′ alternative splicing of transcripts

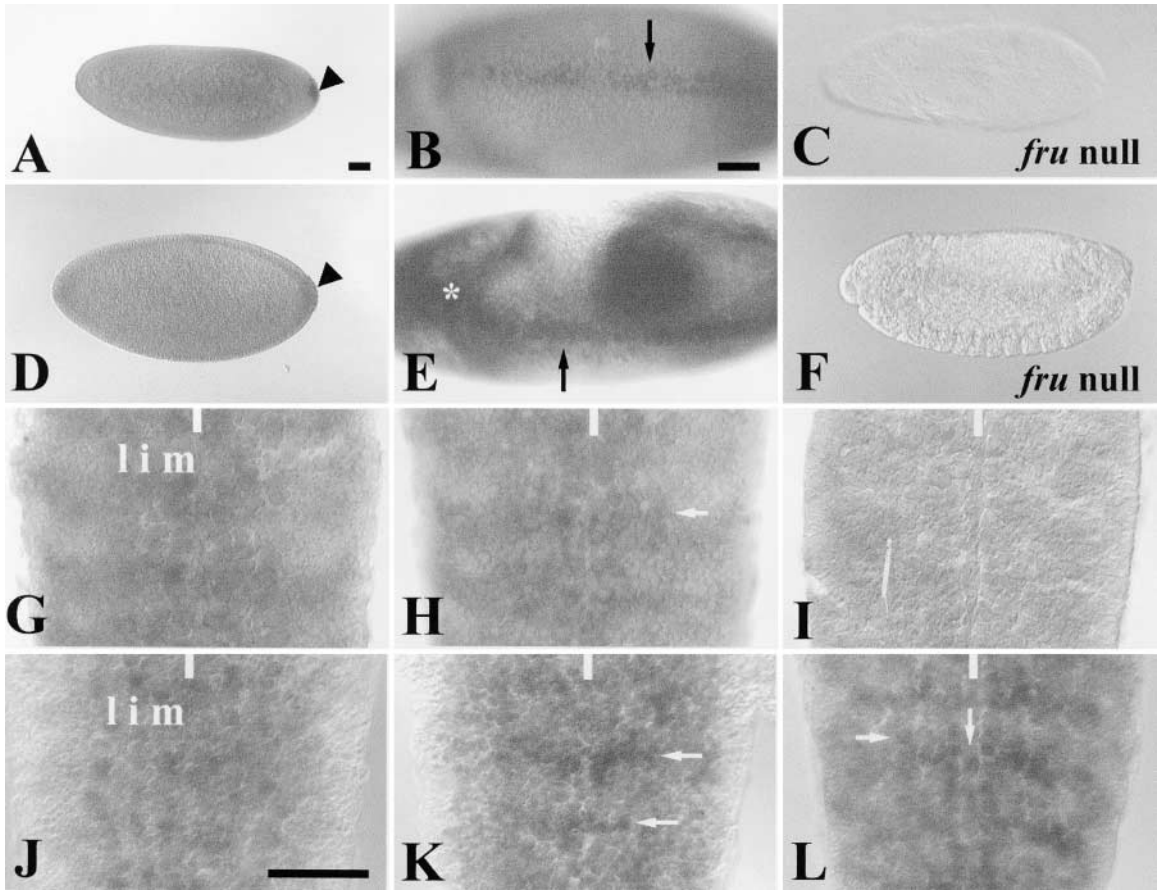

FIGURE 2.—The temporal and spatial distribution of *fru* mRNA and Fru protein. *In situ* hybridization was carried out with digoxigenin-labeled antisense fru^{BTB} riboprobes and AP histochemistry (A–C and G–I). Fru protein distribution was determined by immunohistochemical localization of anti-$Fru^{BTB'}$ followed by AP histochemistry (D–F and J–L). In G–L, embryos were also labeled with anti-Engrailed antibody. (A) Stage 4 wild-type embryo. *fru* mRNA is found in pole cells (arrowhead). (B) Stage 8 wild-type embryo. Mesectodermal cells (arrow) are strongly labeled for *fru* mRNA. (C) Stage 11 *fru* null (fru^{w24}/fru^{w24}) embryo. No *fru* mRNA was detected in any cell types at this stage. (D) Stage 4 wild-type embryo. Fru protein is found in pole cells (arrowhead). (E) Stage 9 wild-type embryo. Cephalic regions (white asterisk) and two rows of mesectodermal cells (arrow; compare with B) express Fru protein. (F) Stage 14 *fru* null (fru^{w24}/fru^{w24}) embryo. No Fru protein was detected in any cell types at this stage. (G) Late stage 9 wild-type embryo. *fru* mRNA is found in three columns of neuroblasts: S1 neuroblasts (l, lateral column and m, medial column) and S2 neuroblasts (i, intermediate column). Engrailed-positive epidermal cells are present in a different focal plane. (H) Stage 10 wild-type embryo. *fru* mRNA appears to be in most GMCs (white arrow) and is also more strongly expressed in the anterior half of the segment. (I) Stage 11 wild-type embryo. *fru* mRNA is present but with less intensity than found in earlier stages. (J) Late stage 9 wild-type embryo. Fru protein is found in three columns of neuroblasts: SI neuroblasts (l, lateral column and m, medial column) and SII neuroblasts (i, intermediate column). (K) Stage 10 wild-type embryo. Fru protein is detected throughout the CNS, appears to be in most or all GMCs (white arrows), and is also more strongly expressed in the anterior half of the segment. (L) Stage 11 wild-type embryo. Fru protein is expressed in a large number of cells in the nervous system. There is slightly stronger expression in many medial neurons, anterior neurons, and cells along the midline. The size of cells (white arrows) and their relative positions indicate that they are likely to be neurons. A–F, whole-mount preparations; G–L, filleted embryo preparations. Vertical white bars (G–L) indicate the ventral midline. Anterior is to the left (A–F) or to the top (G–L). Bars, 20 μm (A and D; B, C, E, and F; and G–I are at the same magnification).

produced from the P2, P3, and P4 promoters is not known. We examined embryos by *in situ* hybridization with three different 3′ end riboprobes to detect transcripts having the A, B, or C 3′ ends (MATERIALS AND METHODS; RYNER *et al.* 1996; GOODWIN *et al.* 2000). Overall, the temporal and spatial expression pattern of transcripts containing the A, B, and C 3′ ends was consistent with the pattern found for *fru* transcripts labeled with antisense-BTB and antisense-Com riboprobes (Table 2A). In the developing CNS, transcripts containing the C 3′ end appeared to be more abundant than those containing the A or B 3′ ends (data not shown). In addition, some tissues, such as the tracheal placodes and amnioserosal cells, were labeled only when riboprobes to the C 3′ end were used, suggesting that there is some tissue-specific regulation of the 3′ alternative splicing of P3 and or P4 *fru* primary transcripts (Table 2A).

To confirm that we were detecting authentic *fru* transcripts, *fru* mutant embryos, fru^{w24}/fru^{w24} and fru^{sat15}/fru^{sat15}, in which the coding regions of the *fru* gene are

TABLE 2

The temporal and spatial distribution of *fru* mRNAs and Fru proteins in embryos

	Antisense riboprobes								
	BTB/Com		*fru* 5′ end probes				*fru* 3′ end probes		
Labeled cell types	CS	Null	P1.S	P2	P3	P4	A	B	C
A. *fru* mRNA distribution[a]									
Preblastoderm stage (st 1–3)	++	++	−	−	+	+	+	+	+
Pole cells (st 4)	++	++	−	−	+	+	+	+	+
Ventral and cephalic furrow (st 5–6)	++	−	−	−	+	+	+	+	+
Mesectoderm (st 7–8)	++	−	−	−	+	+	+	+	+
Neuroectoderm (st 9)	++	−	−	−	+	+	+	+	+
Neuroblast (st 9–10)	++	−	−	−	+	+	+	+	+
Tracheal placodes (st 9–10)	++	−	−	−	+	+	−	−	+
Amnioserosa (st 9–10)	++	−	−	−	+	−	−	−	+
PNS (st 11–16)	−	−	−	−	−	−	−	−	−
CNS (st 11)	++	−	−	−	+	+	+	+	+
CNS (st 12–13)	++	−	−	−	+	+	+	+	+
CNS (st 14–16)	±	−	−	−	−	+	−	−	−

	Antibodies							
	$Fru^{BTB'}$		Fru^{COM}		$Fru^{A'}$		$Fru^{C'}$	
Labeled cell types	CS	Null	CS	Null	CS	Null	CS	Null
B. Fru protein distribution[b]								
Preblastoderm stage (st 1–3)	+	+	+	+	+	+	+	+
Pole cells (st 4)	+	+	+	+	+	+	+	+
Ventral and cephalic furrow (st 5–6)	+	−	+	−	+	−	+	−
Mesectoderm (st 7–8)	+	−	+	−	+	−	+	−
Neuroectoderm (st 9)	−	−	−	−	−	−	−	−
Neuroblasts (st 9–10)	+	−	+	−	+	−	+	−
GMCs (st 10)	+	−	+	−	+	−	+	−
Tracheal placodes (st 10)	+	−	+	−	−	−	+	−
Amnioserosa (st 9–10)	+	−	+	−	−	−	+	−
Midline cells (st 9–11)	+	−	+	−	+	−	+	−
Neurons (st 11/12)	+/+	−	+/+	−	±	−	±	−
CNS neurons (st 13–16)	+	−	+	−	+	−	+	−
PNS neurons (st 13–16)	+	−	+	−	+	−	+	−
CNS Glia (st 13–16)	+	−	+	−	+	−	+	−
PNS Glia (st 13–16)	+	−	+	−	+	−	+	−
Posterior epidermal cell (st 13–16)	+	−	+	−	−	−	+	−
Muscle (st 14–16)	+	−	+	−	−	−	+	−

[a] Wild-type (CS) and *fru* null mutant (homozygous fru^{w24} or fru^{sat15}) embryos were hybridized with digoxigenin-labeled antisense riboprobes and visualized with alkaline phosphatase histochemistry. The intensity of the *in situ* hybridization signal is graded by the number of plus signs in an arbitrary scale; the absence of a detectable signal is indicated by a minus. The data on the temporal and spatial patterns in embryos labeled with the antisense BTB and Com riboprobes were identical and combined within the same column. More than 10 labeled embryos were examined for each stage.

[b] Wild-type (CS) and *fru* mutant (null, homozygous fru^{w24} or fru^{sat15}) embryos were labeled with Fru antibodies and the signal was visualized with AP histochemistry. Fru antibody signals were intensified by treatment with biotinylated tyramide. The presence and relative level of Fru protein histochemical signal is indicated by plus signs and the absence of a detectable signal by minus signs.

deleted, were labeled with the antisense-BTB, antisense-Com, and antisense-A 3′ end riboprobes. At the beginning of embryogenesis, we detected transcripts in these null mutant embryos only up to stage 5; later stage embryos were not labeled (Figure 2, C and F). By contrast, *fru* transcripts in wild-type embryos are present up to stage 16 (Table 2A). From these results, we infer that *fru* transcripts in very early mutant and wild-type embryos are maternally derived, but that the transcripts found only in older wild-type embryos are zygotically

generated. The presence of maternal and zygotic *fru* transcripts was consistent with the results of Fru protein immunohistochemistry (see below).

The temporal and spatial expression of Fru protein during embryogenesis: To determine whether the *fru* transcripts present during embryogenesis are translated, embryos were labeled with antibodies directed against the common coding regions of Fru proteins (anti-Fru^{COM} and anti-Fru$^{BTB'}$) and against the class A 3′ end (anti-Fru$^{A'}$) and the class C 3′ end (anti-Fru$^{C'}$; see MATERIALS AND METHODS). We found that the localization of Fru proteins during embryogenesis is largely consistent with the spatial and temporal RNA distribution described above (Table 2A). Before neuroblast delamination, mesectodermal cells (st 9), but not neuroectodermal cells, were labeled with both anti-Fru^{COM} and anti-Fru$^{BTB'}$ antibodies (Figure 2E; Table 2B). All delaminating neuroblasts and their progeny appear to express Fru proteins (st 9–10; Figure 2J). Ganglion mother cells (GMCs) located in the anterior regions of each segment label more strongly for Fru proteins than do those in the posterior regions (st 10; Figure 2K). At later stages (st 11–16), many cells in the CNS were strongly labeled (Figure 2L).

To determine whether Fru proteins were expressed in neurons and/or glia of stage 13–16 embryos, we carried out double- and triple-labeling experiments with anti-Elav antibodies to identify Fru-positive neurons and with anti-Repo antibodies to identify Fru-positive lateral glia (Figure 3, A and B). From a detailed comparison of double- ($n = 5$) and triple-labeled ($n = 3$) CNSs, it appeared that all Elav-positive cells in the CNS coexpress Fru proteins, even though there were variable levels of Fru protein expression in individual cells (Figure 3C). Likewise, all Repo-positive cells in the CNS were also Fru positive ($n = 5$, Figure 3C). In these experiments, some midline cells were only Fru positive (arrows, Figure 3, C and F). By their location, these cells are likely to be midline glia, which do not express Repo protein (HALTER *et al.* 1995). In summary, all neurons and glia appear to express Fru proteins.

We used antibodies specific to either the A or the C ZnF carboxy termini found in Fru isoforms to determine whether cells have Fru proteins with only one or both of these isoforms (see MATERIALS AND METHODS). The pattern of cells labeled with anti-Fru$^{A'}$ is very similar to the spatial and temporal pattern of cells detected with anti-Fru^{COM} and anti-Fru$^{BTB'}$ (Table 2B). In contrast, in young embryos (st 1–11) the anti-Fru$^{C'}$ labeling pattern is similar to the pattern of cells stained with anti-Fru^{COM} and anti-Fru$^{BTB'}$, whereas at later stages (st 12–16), fewer cells were labeled with anti-Fru$^{C'}$ than with anti-Fru^{COM} and anti-Fru$^{BTB'}$. By double- and triple-labeling experiments in stage 16 embryos, all Elav-positive neurons, Repo-positive lateral glia, and putative midline glial cells were Fru^{A} positive ($n = 4$, Figure 3, D–F). However, all neurons, but only some Repo-positive glia, were Fru$^{C'}$ positive ($n = 5$, Figure 3, G–I). These results suggest that all neurons and some lateral glia contain Fru isoforms having at least two different carboxy termini, but that some lateral glia and midline cells contain Fru proteins that may have only one type of carboxy terminus. Currently, no antibody specific to the B carboxy terminus is available.

In contrast to the findings from the *in situ* hybridization experiments, Fru proteins were detected in neurons and glial cells in the PNS by anti-Fru$^{BTB'}$, anti-Fru^{COM}, anti-Fru$^{A'}$, and anti- Fru$^{C'}$ immunohistochemistry (Figure 3, J–L). In double- and triple-labeling experiments, some Fru-positive cells, labeled with anti-Fru$^{BTB'}$ or anti-Fru^{COM} antibodies, were Elav positive and by location were judged to be mechanosensory and chordotonal organ neurons as well as the more internal multidendritic neurons. Another population of Fru-positive cells were Repo-positive and thus were identified as peripheral glial cells (Figure 3J; Table 2B). However, double- and triple-labeling experiments using anti-Fru$^{A'}$ and anti-Fru$^{C'}$ antibodies showed that only a subset of the Fru-positive sensory neurons and peripheral glia had Fru proteins with the A and C carboxy termini, from which we infer that some of these cells have Fru proteins with the B carboxy terminus (Figure 3, K and L; Table 2B).

Fru proteins are also expressed in other embryonic tissues. The posterior epidermis (st 13–16) and most body wall muscles (st 14–16, Table 2B) were Fru positive by anti- Fru$^{BTB'}$ and anti-Fru^{COM} labeling. These tissues were labeled with anti-Fru$^{C'}$ but not with anti-Fru$^{A'}$ antibodies (Table 2B). These findings suggest that Fru protein isoforms with specific ZnF domains have a tissue-specific pattern in non-CNS tissues. The presence of Fru proteins in cell types that were not labeled in the *in situ* hybridization experiments, such as the PNS or muscle, may be due to differences in sensitivity of the molecular probes used and/or the relative levels of *fru* transcripts and proteins in these different cell types.

To be certain that authentic Fru proteins were being labeled in wild-type embryos, *fru* mutant embryos, fru^{w24}/fru^{w24} and fru^{sat15}/fru^{sat15}, which are deleted for the *fru* gene, were labeled with anti-Fru$^{BTB'}$, anti-Fru^{COM}, anti-Fru$^{A'}$, and anti-Fru$^{C'}$ antibody (Table 2B). At early embryonic stages (st 1–5), the pattern of Fru protein expression in null mutant embryos was comparable to that in wild-type embryos. At later stages (st 6–16), no Fru proteins were detected in null mutant embryos (Figure 2F), even though there was still robust labeling in wild-type embryos. These results indicate that the earliest transcripts present, which we infer to be maternal in origin, are translated in very early stage embryos and that Fru proteins in stage 6–16 embryos are largely or exclusively derived from zygotic *fru* transcripts.

Neurons in the embryonic CNS and PNS are labeled in *fru P*-element lines: To determine whether *P* elements inserted within or near the *fru* locus behave as enhancer traps of the embryonic pattern of *fru* expression, we

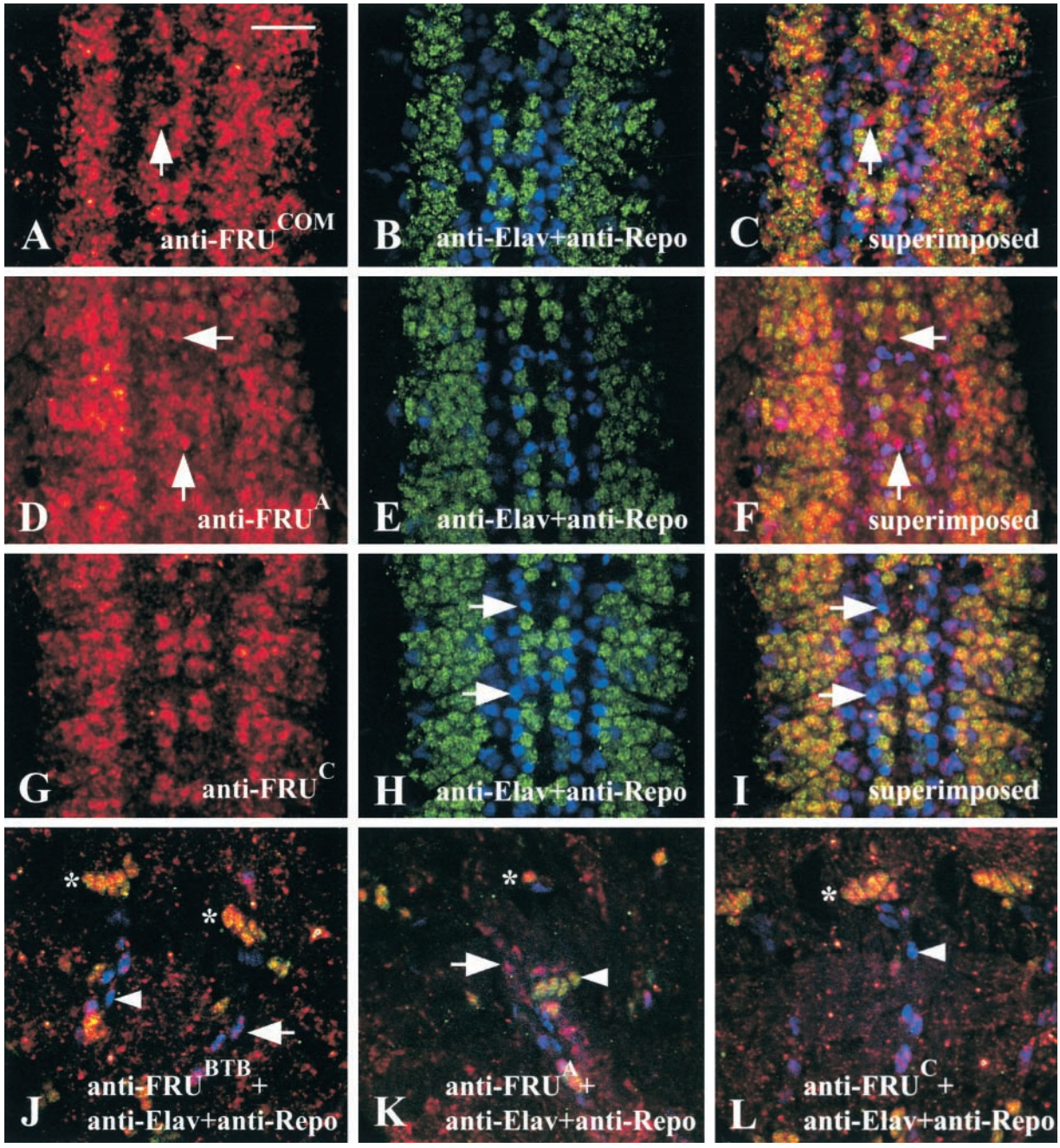

FIGURE 3.—Coexpression of Fru protein with Elav, a neuronal marker, and Repo, a lateral glial marker, in the CNS and PNS. Filleted CNSs from wild-type embryos (st 16) were triple labeled with antibodies to Fru (red), Elav (green), and Repo (blue). A–C, D–F, and G–I are single confocal images in a dorsal CNS focal plane. The images that were merged in Adobe Photoshop are found in C, F, and I. J–L are composite merged images of the lateral body wall from embryos stained as above. (A) CNS cells labeled with anti-Fru^{COM} antibody. The arrow points to a Fru-positive midline cell. (B) CNS cells labeled with anti-Elav and anti-Repo antibodies. (C) In this superimposed image of A and B, all neurons (yellow) and lateral glia (purple) colabel for Fru protein. The arrow points to the same Fru-positive midline cell as in A. (D) CNS cells labeled with anti-Fru$^{A\prime}$ antibody. (E) CNS cells labeled with anti-Elav and anti-Repo antibodies. (F) In this superimposed image of D and E, most neurons (yellow) and glia (purple) colabel for Fru^{A} isoforms. The arrows point to Fru-positive midline cells shown in D. (G) CNS cells labeled with anti-Fru$^{C\prime}$ antibody. (H) CNS cells labeled with anti-Elav and anti-Repo antibodies. Arrows point to two glial cells. (I) In this merged image of G and H, most neurons (yellow) but few glia (purple, arrows in H and I) colabel for Fru^{C} isoforms. (J) All peripheral sensory neurons (asterisk, yellow) are colabeled with anti-Elav and anti- Fru$^{BTB\prime}$ but some glial cells are Fru positive (arrow, purple) and others are Fru negative (arrowhead, blue). The level of Fru expression is low in some sensory neurons and glial cells. (K) A few peripheral sensory neurons (arrowhead and asterisk, yellow) but many glial cells (arrow, purple) label for Fru isoforms that use the A 3′ end. (L) Many peripheral sensory neurons (asterisk, yellow) but only a few glial cells (arrowhead, purple) label for Fru isoforms that use the C 3′ end. Anterior is up for A–I and to the right for J–L. Bar, 20 μm.

examined β-galactosidase activity in fru^3, fru^4, and fru^{sat} mutant and $AJ96w^+$ embryos (Figure 1; Castrillon *et al.* 1993; Ito *et al.* 1996; Spana and Doe 1996). In fru^3, fru^4, and fru^{sat} mutations, a *P* element is inserted between the P2 and P3 promoters (Figure 1; Castrillon *et al.* 1993; Ito *et al.* 1996; Ryner *et al.* 1996; Goodwin *et al.* 2000) and disrupts transcripts from the P1 and P2 *fru* promoters in pharate adult animals (Goodwin *et al.* 2000).

In *fru P*-element mutant and control sibling embryos, cells in the CNS and PNS were labeled by anti-β-galactosidase. Similar temporal and spatial labeling patterns were observed in embryos from the fru^3 and fru^4 lines. In embryos from these lines, anti-β-galactosidase expression was detected in the mesectoderm (st 8), delaminating neuroblasts (st 9; Figure 4, A and B), and a variety of smaller cells, which appear by their location to be GMCs (st 10), neurons (st 11), and lateral glia and midline cells (st 12; Figure 4C). β-Galactosidase labeling persisted in these CNS cells until stage 16. In the embryonic PNS, sensory organ precursors (st 10) followed by the external and chordotonal sensory neurons (st 12–16) were β-galactosidase positive (Figure 4C). In addition, tracheal cells (st 11) and epidermal cells in the posterior part of each hemisegment (st 13–16) were labeled (Figure 4C). By contrast, in embryos from the fru^{sat} line, no β-galactosidase-positive cells were found in the embryonic CNS, and only the chordotonal neurons in the PNS were labeled (data not shown). In summary, these results indicate that β-galactosidase expression from the *P* elements inserted in fru^3 and fru^4 lines largely replicates *fru*'s pattern in the embryonic CNS and PNS.

We also examined the expression pattern of the enhancer trap line $AJ96w^+$. Previous studies have shown that the MP2 neuroblast and its progeny, the dorsal and ventral midline precursor neurons (dMP2 and vMP2), express β-galactosidase in the $AJ96w^+$ line (Spana and Doe 1996). The ventral CNS also showed very weak generalized neuronal expression from stage 14 to 16 and expression in a few lateral sensory neurons (Figure 4D). The generalized ventral nerve cord and sensory neuron labeling in embryos of the $AJ96w^+$ line is similar to the pattern of expression in the $fru^3$and fru^4 lines, but these two *fru* lines did not show prominent MP2 or dMP2/vMP2 neuronal staining.

***fru* function is required for the formation of axonal tracts within the CNS:** Given the findings that the *fru* gene is widely expressed in the embryonic CNS, we expected that *fru* mutant embryos would have defects in CNS development and used two antibodies, anti-FasII and mAb BP102, to assay axonal projections within the CNS. FasII is a neural adhesion molecule expressed on the cell surface of axons forming specific longitudinal fascicles or tracts running throughout the entire ventral nerve cord and into the brain (Figure 5A; Grenningloh *et al.* 1991; Goodman and Doe 1993; Lin *et al.* 1994; Hidalgo and Brand 1997). In whole-mount or flat-dissected preparations of stage 16 and 17 wild-type embryos, three tracts, medial, intermediate, and lateral, are visible in the CNS.

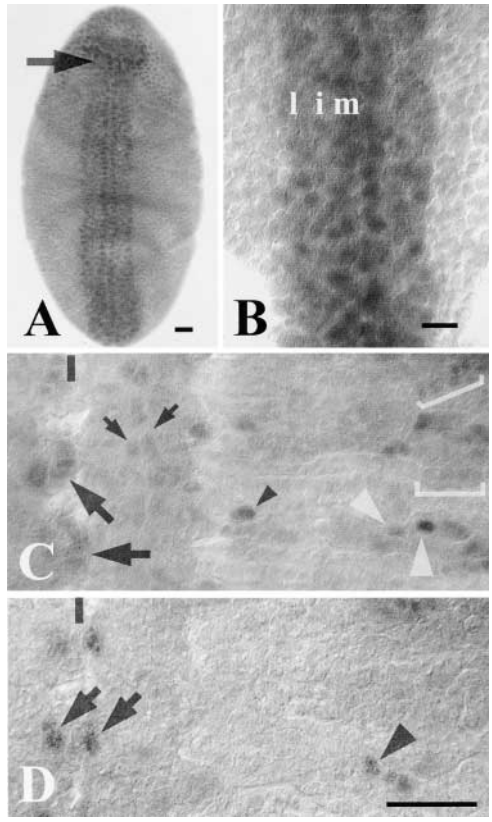

Figure 4.—β-Galactosidase expression pattern in *fru P*-element mutant embryos. Whole-mount embryo (A) or filleted CNSs (B–D) from embryos labeled with anti-β-galactosidase followed by AP histochemistry. (A) Whole-mount fru^4 embryo (stage 9, ventral view). Cephalic (arrow) and ventral neuroblasts strongly express β-galactosidase. (B) Filleted fru^4 embryo (early stage 10, dorsal view). All ventral neuroblasts, including S1 neuroblasts (l, lateral column and m, medial column) and SII neuroblasts (i, intermediate column), are uniformly labeled. (C) Filleted fru^4 embryo (stage 13, composite of dorsal to ventral views to show ventral nerve cord and lateral tissues). At later stages, the expression pattern in the ventral nerve cord shifts to a small number of midline cells (large arrows) and lateral cells, which are likely to be both glia (small arrows) and neurons based on the focal plane. Sensory neurons (white arrowheads), peripheral glia (small black arrowhead), and epidermis (white brackets) also strongly express β-galactosidase. (D) Filleted $AJ96w^+$embryo (stage 13). Two midline neurons, dMP2 and vMP2, are strongly labeled (arrows; Spana and Doe 1996) as are sensory neurons (arrowhead). Vertical black bar (C and D) indicates the ventral midline of embryo. Anterior is up. Bars, 20 μm (C and D, same magnification).

FasII-positive tracts are abnormal in *fru* mutants lacking all or most *fru* transcripts. Between 12 and 25% of *fru* null mutant embryos (*e.g.*, fru^{sat15}/fru^{AJ96u3}) had abnormal FasII-positive tracts (Figure 5, B and C; Table 3D). By comparison, <3% of wild-type embryos had any segments with disrupted FasII tracts (Table 3A). In all

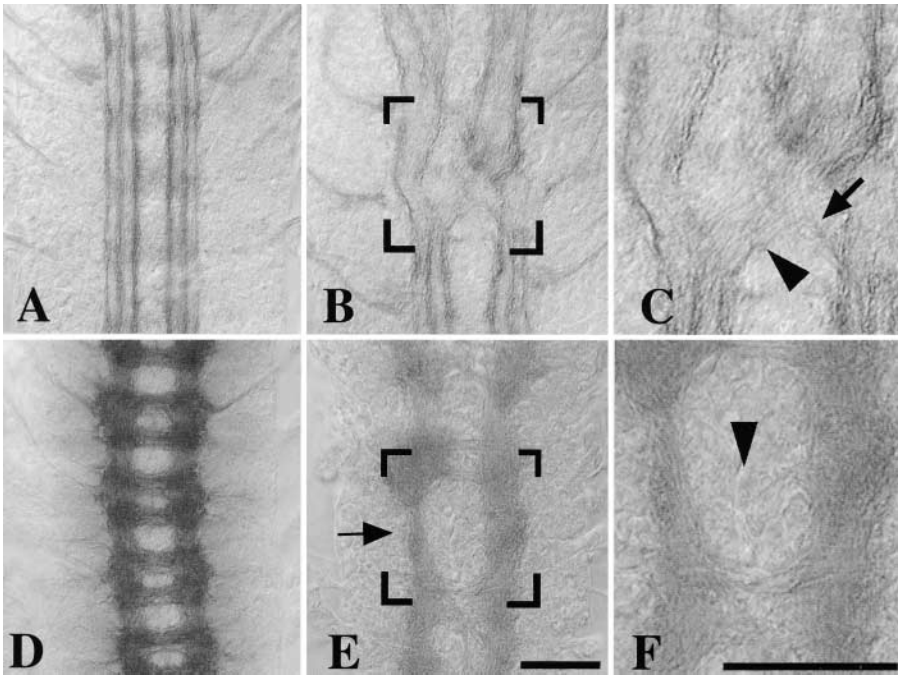

FIGURE 5.—Axonal defects in the CNS of *fru* mutant embryos. Filleted CNSs from wild-type and *fru* mutant embryos (late stage 16) were stained for anti-FasII (A–C) and BP102 (D–F) using HRP histochemistry. (A) In a wild-type embryo, three bilaterally symmetric FasII longitudinal fascicles are visible. (B) In a fru^{w12}/fru^{sat15} embryo, all fascicles within a segment are disrupted. Brackets indicate the area shown at higher magnification in C. (C) Axons in all three fascicles have defasciculated. Axons in the medial MP1 fascicle extend toward the midline (arrowhead and arrow). (D) In a wild-type embryo, BP102-positive axonal processes in each segment form a bilaterally symmetric pair of longitudinal connectives along with the anterior and posterior commissures. (E) In a fru^{w12}/fru^{sat15} embryo, neither the longitudinal connectives (arrow) nor the commissures are uniform in size, suggesting that unequal numbers of axons are present. In some segments (arrow), the commissures are missing. (F) A higher power view of bracketed region in E to show the lack of axonal processes crossing the midline (arrowhead). Bars, 20 μm (A, B, D, and E, same magnification; C and F, same magnification).

fru null mutant CNSs, FasII-positive axons no longer formed distinct tracts in one or more adjacent hemisegment, suggesting that these axons had defasciculated from other axons within the tracts. In some cases, axons that had defasciculated crossed and joined an adjacent fascicle or approached and crossed the midline (Figure 5C). In other cases, the left and right medial tracts appeared to merge along the midline.

To determine whether many or most axonal tracts were disrupted in *fru* mutants, we labeled the longitudinal connectives and commissures with the BP102 antibody (Figure 5D; SEEGER *et al.* 1993). Almost 20% of the *fru* null mutant embryos had defects in the pattern and distribution of BP102-positive axons in the connectives and commissures compared to only 1% of wild-type embryos (Table 3, A and D). Most commonly, in these mutants, the commissures and connectives were not uniform but were either thicker, as though more axons were present, or thinner, as though fewer axons were present (Figure 5, E and F; Table 3, C and D).

To demonstrate that these FasII and BP102 axonal defects depended on the loss of *fru* function, we used the fru^{w12} allele, which has a chromosomal break within the *fru* locus, in combination with *fru* deletion mutations (Figure 1; Table 3C). We found that 15–23% of these mutant embryos had defects in their FasII and BP102 tracts; the frequency and the severity of the defects were similar to those found in *fru* null embryos (Figure 5, B and C). The fru^{w12} allele is caused by a chromosomal inversion, and to rule out the possibility that the non-*fru* inversion breakpoint contributes to the FasII mutant phenotype, we examined $fru^{w12}/Df(3L)XD198$ mutants and found that the pattern of FasII fascicles was wild type ($n = 10$; data not shown; see MATERIALS AND METHODS). These results show that it is the loss of *fru* function that causes the axonal defects in FasII and BP102 tracts (Table 3, C and D). The chromosomal break in the fru^{w12} allele in the *fru* locus separates the P1, P2, and P3 promoters from the *fru* coding region but leaves the P4 *fru* transcription unit intact (ANAND *et al.* 2001). This result suggests that *fru* transcripts from the P1, P2, or P3 promoters are important for wild-type axonal pathfinding.

To further define which *fru* transcripts are required for the formation of FasII and BP102 tracts, we examined *fru* mutants in which P1 transcripts are affected or where P1 and P2 transcripts are eliminated (*e.g.*, $fru^{4\text{-}40}/fru^{sat15}$; Table 3B; ANAND *et al.* 2001). These mutants had wild-type FasII and BP102 axonal tracts and produced P3 and P4 transcripts (Table 3B). The finding that P1 and P2 *fru* transcripts are not required for the formation of FasII and BP102 tracts is consistent with evidence by *in situ* hybridization that these transcripts are not present in embryos (Table 2A). By considering the different *fru* mutant genotypes examined, we infer that expression of P3 and, perhaps, P4 *fru* transcripts is sufficient for the development of wild-type FasII and BP102 tracts. The role of P4 transcripts in this process is inferred

TABLE 3

Analysis of abnormal axonal projections in the CNS of *fru* mutant embryos

Genotypes	% embryos with abnormal FasII (+) fascicles	% embryos with abnormal BP102 label
A. fru^{+} genotype		
Wild type (Canton-S)	3.2 (n = 558)	0.7 (n = 153)
B. *fru* genotypes with reduced P1 or lacking P1 and P2 transcripts but producing P3 and P4 transcripts		
fru^{1}/fru^{w24}	5.2 (n = 135)	3.2 (n = 124)
Cha^{M5}/fru^{sat15}	2.4 (n = 167)	0 (n = 72)
$fru^{4\text{-}40}/fru^{sat15}$	1.6 (n = 316)	3.3 (n = 159)
$fru^{4\text{-}40}/P14$	2.1 (n = 437)	3.6 (n = 111)
C. *fru* genotypes lacking P1, P2, and P3 transcripts		
fru^{w12}/fru^{sat15}	15.0 (n = 176)*	16.3 (n = 151)*
fru^{w12}/fru^{w24}	23.4 (n = 259)*	23.9 (n = 251)*
$fru^{w12}/P14$	20.5 (n = 251)*	ND
fru^{w12}/fru^{AJ96u3}	14.4 (n = 227)*	ND
D. *fru* genotypes producing no *fru* transcripts		
fru^{sat15}/fru^{AJ96u3}	15.8 (n = 133)*	17.4 (n = 190)*
fru^{sat15}/fru^{w24}	12.4 (n = 239)*	18.4 (n = 137)*
$fru^{AJ96u3}/P14$	24.5 (n = 316)*	17.0 (n = 106)*
$P14/fru^{w24}$	25.5 (n = 263)*	ND

The data are presented as the percentage of stage 15/16 embryos (n = total number of embryos) having at least one hemisegment with a defective FasII or BP102 axonal projection. The percentage is the combined average value of two independent labeling experiments. For statistical analysis, one-way ANOVA with genotypes as the main effect revealed significant differences within genotypes labeled with anti-FasII ($F_{12,\ 1706} = 13.09$, $P < 0.0001$) and BP102 ($F_{9,\ 1205} = 20.84$, $P < 0.0001$). Subsequent comparisons (Tukey's HSD) revealed that both FasII staining and BP102 staining in the CNS of *fru* genotypes (identified by an asterisk) were significantly different (all $P < 0.05$) compared to wild type and the viable *fru* genotypes, fru^{1}/fru^{w24}, Cha^{M5}/fru^{sat15}, $fru^{4\text{-}40}/fru^{sat15}$, and $fru^{4\text{-}40}/P14$. ND, not determined.

from data of mutants expressing the fru^{w12} allele and it is possible that P4 transcripts, while present, are not expressed as in wild-type animals (Anand *et al.* 2001).

***fru* function is required for wild-type orientation of pioneering axonal projections:** If the axonal pathfinding defects in *fru* mutants are due to the loss of *fru* function in neuronal precursors or in neurons themselves, then there are two likely explanations for the altered axonal trajectories in these mutants. One explanation is that neurons have not adopted, or only partially adopted, their wild-type identity in *fru* mutants and thus their axons fasciculate with different axonal partners as they grow in the CNS. An alternative explanation is that neurons in *fru* mutants adopt their wild-type identity but are unable to carry out their normal program of axonal pathfinding and differentiation. To distinguish between these two possibilities, we used neuronal and axonal markers to identify the earliest developmental abnormalities in *fru* mutants.

To assess whether *fru* played a role in neuroblast delamination and identity, we first labeled developing neuroblasts with antibodies to the Hunchback (Hb) protein, which labels all delaminating neuroblasts by early stage 9 in wild-type embryos (Figure 6A, n = 10). Fewer neuroblasts were labeled with anti-Hb antibody in early stage 9 fru^{w12}/fru^{sat15} embryos than in wild type, but neuroblasts in all three rows did become Hb positive in late stage 9 embryos (Figure 6, B and C; n = 10 both stages). Thus, the final pattern of Hb expression was wild type in these *fru* mutant embryos but there was a slight temporal delay in either neuroblast delamination itself or the onset of Hb expression in delaminating neuroblasts.

We next examined the development of neurons in *fru* mutants that pioneer the FasII fascicles to better assess whether there were changes in neuronal identity or early defects in axonal differentiation. In the wild-type CNS, pCC, vMP2, dMP2, and MP1 axons initiate the formation of the medial and intermediate FasII tracts within each segment (Hidalgo and Brand 1997; Hidalgo and Booth 2000). The axonal process of the pioneer neurons vMP2 and pCC ascends while the processes of the MP1 and dMP2 axons fasciculate and extend posteriorly. These axons initially produce one fascicle at stage 13, which then splits into two fascicles, the pCC/vMP2 (medial) and dMP2/MP1 (intermediate) fascicles.

We therefore examined the development of aCC, pCC, vMP2, and dMP2 neurons in fru^{sat15}/fru^{AJ96u3} and fru^{w12}/fru^{AJ96u3} embryos. Along the midline, the MP2 precursor expresses the Odd-skipped protein and upon

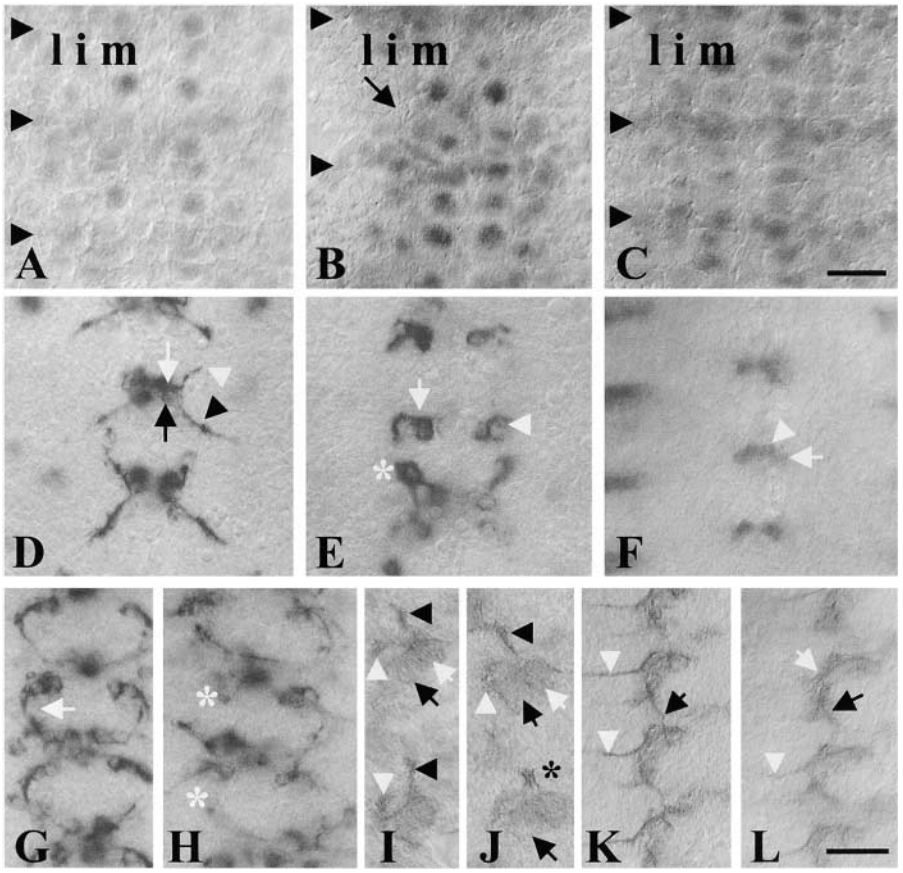

Figure 6.—Neuroblast and neuronal identity and early axonal projections in the CNS of *fru* mutant embryos. Filleted CNSs from wild-type and *fru* mutant embryos labeled with anti-Hunchback (A–C), mab22C10 (D, E, G, and H), anti-Oddskipped (F), and anti-FasII (I–L) antibodies using AP (A–H) or HRP histochemistry (I and J). (A) Early stage 9 wild-type CNS. Full complement of Hb-positive NBs in medial (m), intermediate (i), and lateral (l) columns. Rows of En-positive cells (arrowheads) indicate the position of posterior compartments in A–C. (B) Early stage 9 fru^{w12}/fru^{w24} CNS. Fewer Hb-positive neuroblasts (arrow) are found at this stage than in wild-type embryos. (C) Late stage 9 fru^{w12}/fru^{w24} CNS. Hb-positive neuroblasts in all columns are present in a pattern similar to that in wild-type embryos. (D) Midstage 12 wild-type CNS. The mab22C10-positive vMP2 neuron (white arrow) projects its axon anteriorly (white arrowhead) and the dMP2 neuron (arrow) initially projects its axon posteriorly (arrowhead). (E) Midstage 12 fru^{w12}/fru^{sat15} CNS. vMP2 and dMP2 neurons often do not express mab22C10 as strongly as does wild type. In some segments, mab22C10-positive neurons were not in their typical anterior-posterior location (indicated by asterisk) and had delayed outgrowth of axonal processes (white arrowhead). The white arrow points to a cell with an abnormally oriented growth cone. (F) Midstage 12 fru^{w12}/fru^{sat15} CNS. Odd-skipped-positive vMP2 (white arrowhead) and dMP2 (white arrow) neurons are present in the *fru* mutant embryo. (G) Early stage 13 wild-type CNS. Initial axonal outgrowth forming the mab22C10 medial fascicle (white arrow). (H) Early stage 13 fru^{w12}/fru^{sat15} CNS. The medial fascicle (asterisks) is not yet formed. (I) Midstage 12 wild-type CNS. FasII-positive aCC neuron (white arrow) extends its axon peripherally (white arrowhead) and the FasII-positive pCC neuron (arrow) projects its axon anteriorly (arrowhead). (J) Midstage 12 $fru^{w12}/P14$ CNS. In the more anterior hemisegment, the FasII-positive aCC neuron (white arrow) extends its axonal growth cones toward the periphery (white arrowhead) and the pCC neuron (arrow) sends its axon anteriorly (arrowhead). In the other hemisegment both aCC and pCC axons extend anteriorly (asterisk). (K) Early stage 13 wild-type CNS. The developing FasII medial fascicle (arrow) is well organized. All aCC neurons have extended their axons posteriorly (white arrowheads). (L) Early stage 13 $fru^{w12}/P14$ CNS. The developing FasII medial fascicle (arrow) is indistinct, suggesting that the axons are not as fasciculated as those in wild type. In one hemisegment, the FasII-positive aCC axon (white arrow) extends posteriorly, not toward the periphery. Other aCC axons (white arrowhead) extended to the periphery. Anterior is to the top. The midline is to the right (I–L). Bars, 20 μm (A–C, same magnification; D–L, same magnification).

division the dMP2 daughter cell maintains Odd-skipped expression while the vMP2 daughter downregulates Odd-skipped expression (Broadus *et al.* 1995; Spana and Doe 1996). In *fru* mutant embryos all segments had the expected complement of Odd-skipped neurons along the midline (Figure 6F; fru^{w12}/fru^{AJ96u3} and fru^{sat15}/fru^{AJ96u3}, $n = 35$ segments, $n = 5$ embryos of each genotype). The other pioneer neurons, aCC and pCC neurons, can be recognized by their location and FasII expression in stage 12 embryos (Figure 6I; Grenningloh *et al.* 1991). In *fru* mutant embryos, aCC and pCC neurons were present and beginning to extend their axonal processes (Figure 6J). These results show that in *fru* mutant embryos, neurons pioneering the medial and intermediate FasII tracts express markers appropriate for their expected neuronal fate.

To assess the early outgrowth of axons from these neurons as they begin to differentiate their axons, we labeled neurons with markers to assess axonal outgrowth. The mab22C10 antibody recognizes the *futsch* protein, which labels the vMP2 and dMP2 axons and is needed for the normal outgrowth of axonal processes (Figure 6D; Hummel *et al.* 2000). In *fru* mutant embryos (st 12), the somas and axons of vMP2 and dMP2 neurons were strongly labeled in only 20–33% of the hemisegments (Figure 6E; 10/50 hemisegments, $n = 16$ fru^{w12}/fru^{AJ96u3} embryos; 28/84 hemisegments, $n = 20$ fru^{sat15}/fru^{AJ96u3} embryos). Every *fru* mutant embryo examined had hemisegments in which neither the dMP2 or vMP2 cell body nor their axonal processes were labeled (Figure 6E) whereas 92% of the wild-type embryos had heavily labeled neurons (Figure 6D; $n = 100$ hemisegments,

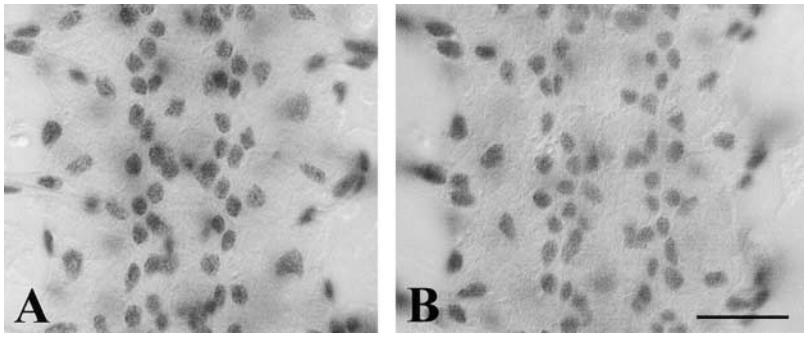

FIGURE 7.—Repo-positive glial cells are present in the *fru* mutant CNS. Filleted CNSs from wild-type and *fru* mutant embryos were labeled with anti-Repo antibody and visualized with nickel-enhanced HRP histochemistry. (A) Stage 14 wild-type CNS. A regular array of longitudinal glia are present. (B) Stage 14 fru^{w12}/fru^{sat15} CNS. The number of longitudinal glia present is similar to that found in wild-type CNS but the glial cells are more distributed in the mutant. Anterior is to the top. Bar, 20 μm.

13 embryos). In those mab22C10-positive dMP2 and vMP2 neurons in which the initial outgrowth of axonal growth cones could be determined, axonal outgrowth was delayed or, if present, the growth cone appeared to be initiating growth in an abnormal direction (Figure 6E). At slightly later stages (st 13), many of these mab22C10-positive dMP2 and vMP2 axons had not yet formed the medial fascicle or if the fascicle was present its organization was abnormal (Figure 6H) compared to the developing medial fascicle in wild-type embryos (Figure 6G). FasII-positive axons also contribute to the medial fascicle and in *fru* mutants these axons do not form distinct fascicles as found in wild type (compare Figure 6K to 6L). Early axonal outgrowth of the FasII aCC motorneurons occasionally fails to initially grow toward the periphery, either joining the ascending pCC axon (Figure 6J) or growing posteriorly (Figure 6L). These findings show that the initial emergence of the growth cones from these pioneer neurons is delayed or abnormal in *fru* mutants.

***fru* function is not required for lateral and midline glial cell survival:** The axonal phenotypes in *fru* mutant embryos might also result from the loss of midline or lateral glial cells, both of which have been shown to be necessary for the formation of normal axonal tracts and to express Fru proteins (Figure 3, C, F, and I; HALTER *et al.* 1995; GIESEN *et al.* 1997; SCHOLZ *et al.* 1997; HUMMEL *et al.* 1999). We examined *fru* mutant embryos to determine if both types of glia were present in the appropriate numbers and locations within the CNS. In fru^{w12}/fru^{sat15} embryos, the average number of Repo-positive glial cells (Figure 7B; 44 ± 4 glia/neuromere, $n = 4$) was not different from that in wild-type embryos (Figure 7A; 45 ± 4 glia/neuromere, $n = 4$; $P > 0.05$, two-sample *t*-test). The pattern of Repo-positive glial cells was slightly abnormal in *fru* mutants (Figure 7B). To label midline glial cells, the AA142 enhancer trap *P* element was recombined onto the fru^{sat15} and fru^{AJ96u3} chromosomes (SCHOLZ *et al.* 1997). *fru* mutant embryos had a wild-type pattern of three to four midline glial cells expressing β-galactosidase ($n = 5$, fru^{w12}/fru^{AJ96u3}; $n = 6$, fru^{sat15}/fru^{AJ96u3} embryos). Since wild-type numbers of glial cells are present in *fru* mutants, it does not appear that *fru* is required for the survival of glial cells. Thus the defects in the FasII and BP102 axonal tracts do not appear to be due to a loss of midline or lateral glia.

The expression of specific *UAS-fru* transgenes rescues mutant defects in the CNS of *fru* mutant embryos: The phenotypic analysis of *fru* mutant embryos along with *fru*'s temporal and spatial expression pattern suggests that the *fru* gene functions during axonal outgrowth. To positively demonstrate *fru*'s role in the CNS, we rescued *fru* mutant defects by the expression of *UAS-fru* transgenes controlled by a pan-neuronal driver, *scabrous* (*sca*)*-GAL4* (BRAND and PERRIMON 1993). The expression pattern of the *sca-GAL4* driver line used was confirmed with a *UAS-lacZ* reporter transgene; uniform β-galactosidase expression was found first in the neuroectoderm, followed by expression in neuroblasts, GMCs, and neurons through stage 16 (KLAES *et al.* 1994; data not shown). This pattern mirrors Fru's expression pattern in the CNS (see above). We generated three different *fru* constructs that encode the same BTB and Common sequences but differ in which one of the three 3′ ZnF domain sequences was included; these constructs are designated as *UAS-fruA*, *UAS-fruB*, and *UAS-fruC* (see MATERIALS AND METHODS).

The expression of *UAS-fruA* and *UAS-fruC* transgenes under the control of a *sca-GAL4* driver was sufficient to rescue the defects in FasII and BP102 axonal tracts in *fru* mutant embryos (Figure 8, A, C, D, and F; Table 4). Embryos from two lines with independent *UAS-fruA* and *UAS-fruC* insertions in the fru^{w12}/fru^{sat15} mutant background were examined (Figure 8, A and C; Table 4). In both lines of *sca-GAL4/UAS-fruA*; fru^{w12}/fru^{sat15} embryos, the wild-type BP102 pattern was also restored (Figure 8D; Table 4). However, the BP102 pattern was rescued in embryos from only one of the *UAS-fruC*; *sca-GAL4;* fru^{w12}/fru^{sat15} lines (Figure 8F); in the other line, 33% of *fru* mutant embryos had an abnormal BP102 pattern (Table 4).

In contrast to the results obtained from expressing the *UAS-fruA* and *UAS-fruC* transgenes, the FasII and BP102 mutant phenotypes were more severe in the CNSs of *sca-GAL4/UAS-fruB*; fru^{w12}/fru^{sat15} embryos than in the CNSs of the corresponding *fru* mutants (Tables 3C and 4). The FasII labeling in the CNS of these embryos was diffuse, indicative of highly defasciculated axonal pro-

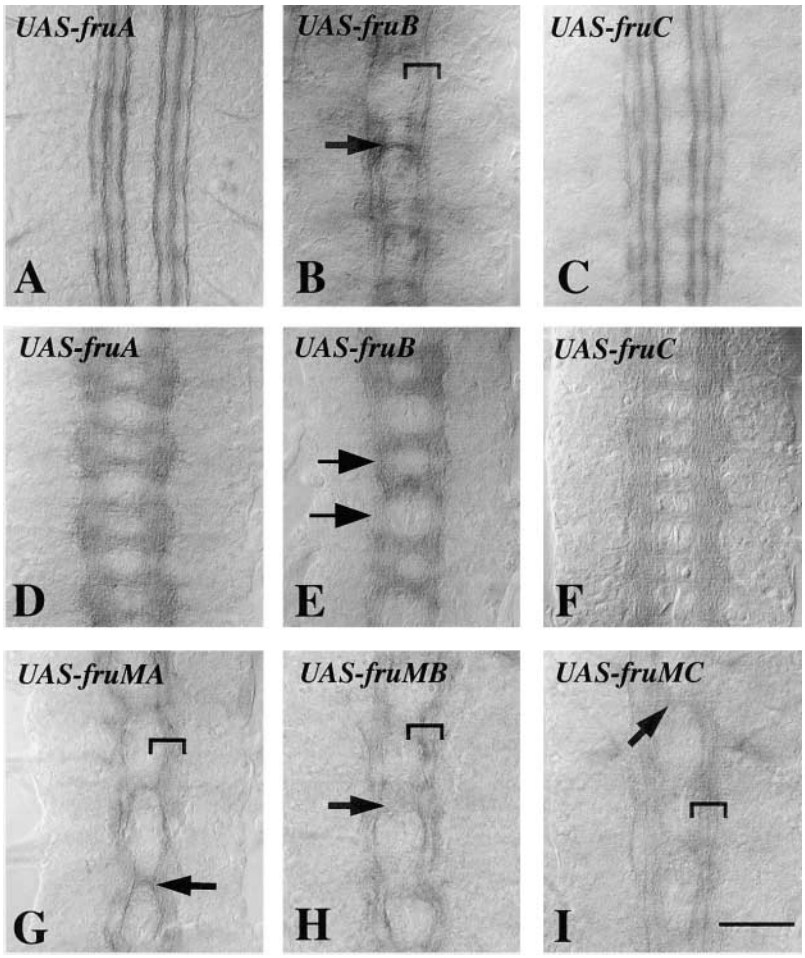

FIGURE 8.—The expression of specific *fru* transgenes rescues the axonal defects in FasII- and BP102-positive axons in *fru* mutants, but the expression of male-specific *fru* transgenes disrupts axonal tracts in the CNS. Filleted CNS from fru^{w12}/fru^{sat15} embryos (st 16) expressing a *UAS-fru* or *UAS-fruM* transgene under the control of the *sca-GAL4* driver was labeled for anti-FasII (A–C and G–I) or BP102 (D–F) followed by HRP histochemistry. (A) CNS of *fru* embryo expressing the *UAS-fruA* transgene. All segments have a normal pattern of FasII tracts. (B) CNS of *fru* embryo expressing the *UAS-fruB* transgene. All segments have a more abnormal pattern of FasII tracts (bracket) than does the fru^{w12}/fru^{sat15} mutant embryo alone (see Figure 5B). In addition, many axons project across the midline (arrow). (C) CNS of *fru* embryo expressing the *UAS-fruC* transgene. All segments have a normal pattern of FasII tracts. (D) CNS of *fru* mutant embryo expressing the *UAS-fruA* transgene. All segments have a normal pattern of BP102-positive longitudinal connectives and commissures. (E) CNS of *fru* embryo expressing the *UAS-fruB* transgene. Many segments have a pattern of BP102-positive longitudinal connectives and commissures slightly more abnormal than that of wild type. (F) CNS of *fru* mutant embryo expressing the *UAS-fruC* transgene. All segments have a normal pattern of BP102-positive longitudinal connectives and commissures. (G) CNS of *fru* embryo expressing the *UAS-fruMA* transgene. All segments have defasciculated (bracket) and midline crossing (arrow) FasII-positive axons. (H) CNS of *fru* embryo expressing the *UAS-fruMB* transgene. All segments have defasciculated (bracket) and midline crossing (arrow) FasII-positive axons. (I) CNS of *fru* embryo expressing the *UAS-fruMC* transgene. All segments have defasciculated (bracket) and midline crossing (arrow) FasII-positive axons. Anterior is up. Bar, 20 μm.

jections, and axons frequently crossed between fascicles or across the midline (Figure 8B; Table 4). Not surprisingly, the BP102 pattern in both lines of *sca-GAL4/UAS-fruB*; fru^{w12}/fru^{sat15} embryos was also severely disrupted (Figure 8E; Table 4). Sibling embryos, *sca-GAL4/UAS-fruB*; fru^{-}/fru^{+}, also had had defective FasII and BP102 axonal tracts (95% embryos, $n = 20$, figure not shown). Taken together, these results indicate that the *sca-GAL4*-driven expression of *UAS-fruB* may be exerting a dominant negative effect on the development of these FasII and BP102 axonal phenotypes. In addition, the defects in mab22C10-positive axons in the dMP2 and vMP2 pioneer neurons in *UAS-fruA*, *UAS-fruB*, or *UAS-fruC* fru^{w12}/fru^{sat15} mutants were not rescued ($n = 50$ hemisegments of *fru* mutant embryos expressing each construct; data not shown).

To determine whether Fru function in postmitotic neurons might be sufficient to restore wild-type FasII tracts in *fru* mutants, we used an *elav-GAL4* driver to express the *UAS-fru* transgenes (LIN and GOODMAN 1994). In every case, the mutant phenotypes were not rescued; rather, more embryos developed defective FasII tracts and individual embryos had more affected hemisegments than were found in the *fru* mutant genotype alone (Table 5). These findings suggest that *fru* transgene expression solely in neurons is insufficient to restore normal FasII axonal phenotype in *fru* mutant embryos and interferes with the development of normal pathfinding by FasII axons.

The male-specific transcripts of *fru* derived from the P1 promoter encode an additional N-terminal extension to the common coding sequences of most *fru* transcripts but are not expressed in the embryo (Table 2A; ITO *et al.* 1996; RYNER *et al.* 1996; USUI-AOKI *et al.* 2000). To ask if these P1 *fru* transcripts might also be able to rescue the defective axonal projections in *fru* mutants, we used three *fru* constructs derived from male-specific *fru* cDNAs (see MATERIALS AND METHODS). These constructs, designated as *fruMA*, *fruMB*, and *fruMC*, were made from the sequences encoding the 101 male-spe-

TABLE 4

Pattern of FasII and BP102 axonal tracts in *fru* mutants expressing *UAS-fru* transgenes in the CNS: the *fru* transgene expression by *scabrous-GAL4*

	UAS-fru constructs driven by *sca-Gal4*		
Phenotypes examined	*fruA*	*fruB*	*fruC*
% of embryos with an abnormal FasII pattern	7.1 ($n = 42$)[a]	92.6 ($n = 94$)[b]	7.6 ($n = 105$)[a]
	5.9 ($n = 51$)[c]	96 ($n = 90$)[c]	7.6 ($n = 105$)[c]
% of embryos with an abnormal BP102 pattern	4.5 ($n = 44$)[a]	99 ($n = 116$)[b]	2.5 ($n = 118$)[a]
	4.4 ($n = 45$)[c]	100 ($n = 34$)[c]	33.3 ($n = 84$)[d]
	UAS-fruM constructs driven by *sca-Gal4*		
Phenotypes examined	*fruMA*	*fruMB*	*fruMC*
% of embryos with an abnormal FasII pattern	100 ($n = 113$)[e]	100 ($n = 123$)[e]	93.9 ($n = 115$)[e]
	99 ($n = 63$)[c]	94 ($n = 50$)[c]	98.1 ($n = 53$)[c]
% of embryos with an abnormal BP102 staining	100 ($n = 115$)[e]	100 ($n = 125$)[e]	96.8 ($n = 156$)[e]
	100 ($n = 36$)[c]	94 ($n = 47$)[c]	93 ($n = 43$)[c]

The percentage of stage 15/16 *w; fru^{w12}/fru^{sat15}; sca-GAL4; UAS-fru* transgenic embryos with defective FasII or BP102 pattern was determined. This percentage is an average of two independent experiments in which whole-mount embryos were evaluated for their mutant phenotype. For most comparisons, data from only one line were included in the statistical analysis. A one-way ANOVA, which included data from Table 3, showed significant differences among genotypes in the number of embryos with abnormal FasII ($F_{17, 45291} = 281$, $P < 0.0001$) and BP102 tracts ($F_{14, 45539} = 441$, $P < 0.0001$). Subsequent comparisons (Tukey's HSD) were made among fru^{w12}/fru^{sat15} mutants, wild type, and *fru* mutants expressing *UAS-fru* transgenes.

[a] The FasII patterns of *UAS-fruA/sca-GAL4;* fru^{w12}/fru^{sat15} and *UAS-fruC/sca-GAL4;* fru^{w12}/fru^{sat15} embryos were not different from the patterns in wild-type embryos. However, the frequency of the FasII defects in *fru* mutant embryos expressing the transgenes *UAS-fruA* and *UAS-fruC* were significantly different from the frequency of FasII defects found in fru^{w12}/fru^{sat15} embryos. The percentage of *UAS-fruA/sca-GAL4;* fru^{w12}/fru^{sat15} and *UAS-fruC/sca-GAL4;* fru^{w12}/fru^{sat15} embryos with a defective BP102 pattern was not significantly different from that found in wild-type embryos but was different from the percentage of fru^{w12}/fru^{sat15} embryos with defects in their BP102 pattern.

[b] The percentage of *UAS-fruB/sca-GAL4;* fru^{w12}/fru^{sat15} embryos with an abnormal FasII pattern or an abnormal BP102 pattern was significantly different from the percentage of defects found in wild-type and fru^{w12}/fru^{sat1} embryos.

[c] The data from the second line for each transgene are included in the table but were not statistically analyzed.

[d] The percentage of affected embryos labeled for BP102 was discordant between the two transformant *w;* fru^{w12}/fru^{sat15}; *sca-GAL4; UAS-fruC* lines. A separate one-way ANOVA was calculated for the analysis of the BP102 staining in this line and showed significant differences among genotypes in the number of embryos with abnormal BP102 tracts ($F_{14, 45292} = 435$, $P < 0.0001$). Subsequent comparisons (Tukey's HSD) showed that this line was different both from wild type and from *fru* mutant alone ($P < 0.05$).

[e] The frequency of defects in both FasII and BP102 tracts in mutant embryos expressing any of the *UAS-fru* male transgenes was significantly different from the frequency of defects in both wild-type and *fru* mutant embryos.

cific amino termini and the BTB and Common coding sequences and had sequences for one of the three different 3′ ends. The FasII- and BP102-positive axonal tracts were defective in virtually all *UAS-fruMA/ sca-GAL4;* fru^{w12}/fru^{sat15}, *UAS-fruMB/ sca-GAL4;* fru^{w12}/fru^{sat15}, and *UAS-fruMC / sca-GAL4;*fru^{w12}/fru^{sat15} embryos (Figure 8, G–I; Table 4). In these embryos, FasII axons were defasciculated and often crossed the midline (Table 4). Thus, the male-specific *UAS-fruM* transgenes interfered globally with axonal patterning, suggesting that these *fru* male-specific proteins are unable to function in the same way as the Fru proteins encoded by other *fru* promoters.

DISCUSSION

***fru* transcripts and proteins are expressed during embryogenesis:** This is the first report showing that *fru* transcripts and proteins are expressed during embryogenesis (but see Zollman *et al.* 1994; Lee *et al.* 2000). Fru proteins are present in neuronal precursors, neuroblasts (NBs), GMCs, and their progeny, neurons and glia. Furthermore, using promoter-specific riboprobes for *in situ* hybridization, we have shown that the *fru* transcripts in the embryo are generated from the P3 and P4 promoters, but not from the P1 or P2 promoters. The presence of *fru* transcripts at very early embryonic stages suggests that at least some *fru* transcripts are likely to be produced maternally and then sequestered in the oocyte (M. Foss and B. J. Taylor, personal communication).

The presence of multiple isoforms and tissue-specific patterns of expression are common characteristics of the BTB/POZ-ZnF transcription factor family. For example, the *tramtrack* (*ttk*) gene encodes two isoforms, Ttkp69 and Ttkp88, that are expressed in the CNS and

TABLE 5

Pattern of FasII and BP102 axonal tracts in *fru* mutants expressing *UAS-fru* transgenes in the CNS: the *fru* transgene expression by *elav-GAL4*

	UAS-fru constructs driven by *elav-Gal4*		
Phenotypes examined	*fruA*	*fruB*	*fruC*
% of embryos with an abnormal FasII pattern	70.6 (n = 51)	93.2 (n = 59)	67.8 (n = 56)

The percentage of stage 16 *elav-GAL4;UAS-fru;* fru^{w12}/fru^{sat15} transgenic embryos with defective FasII was determined. None of the *fru* transgene expressed only in postmitotic neurons rescued the defects in the FasII phenotypes, suggesting that neuronal expression only of transgenes is not sufficient to restore mutant phenotypes to normal.

PNS. The Ttkp69 protein is expressed in CNS glial cells and Ttkp88 is expressed in the peripheral nervous system (Giesen *et al.* 1997); Ttkp69 has been implicated in the formation of wild-type axonal tracts in the CNS (Giesen *et al.* 1997). Another gene with a similar structure to *fru* is the *Broad-Complex* (*BR-C*) in which a family of BTB/POZ-ZnF transcription factors is encoded by a single primary transcript that is spliced into four transcripts sharing a common 5′ end spliced alternatively to 3′ sequences encoding one of four pairs of C_2H_2 zinc-finger domains (Z1, Z2, Z3, and Z4; Bayer *et al.* 1997). Phenotypic analysis of *BR-C* mutants, in which the expression of individual isoforms is disrupted, has led to the proposal that certain isoforms have specific functions. For example, the Z1 isoform mediates the *reduced bristle on palpus* wild-type function and the Z2 isoform mediates the *broad* wild-type function (DiBello *et al.* 1991; Sandstrom *et al.* 1997). Although all tissues during metamorphosis appear to contain all *BR-C* isoforms, the relative abundance of the different isoforms is tissue specific and is thought to contribute to tissue specificity in the response to ecdysone (Restifo and Merrill 1994; Bayer *et al.* 1997; Restifo and Hauglum 1998).

Compared to these BTB/POZ-ZnF genes, the *fru* gene has additional complexity, including multiple promoters as well as alternative 5′ and 3′ end splicing. This transcript complexity means that tissue- and stage-specific gene expression may be regulated by the choice of the promoter as well as alternative splicing. In the best-understood example of *fru* transcript regulation, P1 *fru* transcripts are expressed in the CNS from late larval through adult stages and show sex-specific splicing at the 5′ end of the primary transcript and sex-nonspecific alternative splicing of the 3′ ends (Goodwin *et al.* 2000; Usui-Aoki *et al.* 2000; S. F. Goodwin, L. C. Ryner, T. Carlo, M. Foss, J. C. Hall, B. J. Taylor and B. S. Baker, unpublished results). The outcome of this sex-specific splicing regulation is the translation of P1 transcripts in males but not in females (Lee *et al.* 2000; Usui-Aoki *et al.* 2000).

For the other *fru* transcripts derived from the P2, P3, and P4 promoters, little is known of their regulation. Our results suggest that in the CNS most or all neurons and glia express transcripts derived from both the P3 and P4 promoters. The finding that transcripts having any one of the three different 3′ ZnF domains are also widely expressed suggests that neurons and glia likely coexpress multiple Fru isoforms with different ZnF domains. If both P3 and P4 transcripts are spliced to use the full range of alternative 3′ ends, there may be as many as six different *fru* transcripts within individual neurons or glia. These alternative 3′ ends encode peptides that differ in size as well as in the position and sequence of the ZnF domain (Goodwin *et al.* 2000; Usui-Aoki *et al.* 2000). Thus, most or all CNS neurons and glia appear to have multiple Fru isoforms but it is not known whether these proteins will have different functions. In only a few embryonic cell types, such as skeletal muscle, peripheral neurons, and glia, was there evidence from immunohistochemical analysis for isoform-specific expression of Fru proteins.

Our finding of a good correspondence between the cell types that were β-galactosidase positive in the fru^3 and fru^4 *P*-element lines and the pattern of Fru antibody labeling suggests that enhancers sufficient to control *fru*'s embryonic expression pattern are located in nearby regions. The similarity in the pattern of label in the fru^3 and fru^4 lines indicates that these embryonic enhancers are likely to be distributed in the 40-kb region between the relevant *P*-element insertion sites located between the P2 and P3 promoters (Goodwin *et al.* 2000). By comparison, the number and pattern of labeled cells in the fru^{sat} and fru^4 lines are not identical, even though their *P* elements are inserted in essentially the same genomic location, suggesting that either intrinsic features of these *P* elements or their orientation affects reporter gene expression (Goodwin *et al.* 2000).

The formation of longitudinal and commissural tracts in the embryonic CNS depends on *fru* function: Our results show that the *fru* gene has sex-nonspecific functions in the development of the embryonic axonal scaffold. *fru* mutants that lack most or all *fru* transcript classes formed longitudinal and commissural axonal tracts in which axons did not coalesce into fascicles, fasciculated with inappropriate partners, or were unable to maintain proper fasciculation. Consistent with the *in*

situ hybridization experiments, *fru* mutants, in which P1 or P1 and P2 transcripts were disrupted, formed wild-type FasII and BP102 tracts. By contrast, in *fru* mutants where P1, P2, and P3 transcripts were disrupted, but P4 transcripts were present, the defects in FasII and BP102 axonal tracts were as severe as the defects in embryos completely lacking *fru* function. Consideration of the axonal phenotypes in these different *fru* mutant genotypes suggests that P3 *fru* transcripts are sufficient for the formation of wild-type FasII and BP102 tracts. Even though this explanation is the simplest that accounts for our data, we are unable to assess the effects of the loss of transcripts from only the P2, P3, or P4 promoter. Thus, we are unable to rule out the possibility that elimination of other *fru* transcripts or combinations of transcripts might also result in defective axonal pathfinding.

The embryonic phenotypes of complete loss of *fru* mutants are mild with only a fraction of mutant embryos showing defects in their axonal tracts. This relatively benign phenotype suggests that the activity of other genes may be able to compensate for the loss of *fru* function. Mutants in other genes, such as *fasII*, *Dlar*, and other receptor protein tyrosine phosphatases that encode fasciculation and guidance molecules, also exhibit weak phenotypes in single mutants but show much stronger phenotypes in double mutants or when heterozgyous with mutations that reduce the function of genes that operate in the same developmental pathway (Grenningloh *et al.* 1991; Seeger *et al.* 1993; Krueger *et al.* 1996; Sun *et al.* 2000).

***fru* expression in the embryonic CNS rescues axonal pathfinding defects in *fru* mutants:** The widespread expression of the *fru* gene in neurons and lateral and midline glia suggests that its function may be required in each of these three cell types and that it influences a variety of cellular processes necessary for the formation of a wild-type axonal scaffold. Each of these three cell types has been shown to function during the creation of the wild-type axonal scaffold (Klämbt 1993; Giniger *et al.* 1994; Hummel *et al.* 1999; Tear 1999; Hidalgo and Booth 2000). We found that the expression of *fru* transgenes in neuronal precursors and neurons, producing proteins similar to those encoded by P3 and P4 *fru* transcripts, rescued axonal pathfinding defects in *fru* mutants. Expression of the *UAS-fruA* and *UAS -fruC* transgenes controlled by the *sca-GAL4* driver provided the most effective rescue of the *fru* mutant FasII and BP102 axonal phenotypes, suggesting that these transgenes encode Fru isoforms with very similar functions.

By contrast, the *UAS-fruB* transgene did not rescue the mutant axonal phenotypes when expressed with the same pan-neuronal *sca-GAL4* driver, but instead led to an increase in the severity and frequency of abnormal FasII and BP102 tracts. The simplest explanation for these results is that the FruB isoform, unlike the FruA and FruC isoforms, is not able to functionally replace other Fru isoforms. The increased severity of the phenotypes in these embryos suggests that the FruB isoform may interfere, perhaps as a dominant negative factor, with the function of the FruA and/or FruC isoforms or with other proteins involved in axonal pathfinding. Alternately, *sca-GAL4*-driven FruB expression may not replicate the wild-type temporal or spatial pattern or expression level of FruB proteins and these differences in expression may be responsible for the exacerbated axonal phenotypes. Furthermore, our results also show that the misexpression of all of the male-specific Fru isoforms leads to an increased severity in the FasII and BP102 mutant phenotypes of *fru* mutant and control sibling embryos. Since embryos do not normally produce these Fru^M proteins, the ectopic expression of these Fru^M proteins appears to interfere with the function of one or more of the other Fru isoforms or with the activity of proteins needed for wild-type axonal pathfinding.

In contrast, the expression of *fru* transgenes in postmitotic neurons by the *elav-GAL4* driver failed to rescue *fru* mutant axonal phenotypes. This failure to rescue suggests that the *fru* gene may function at earlier stages in neuronal development, such as in neuroblasts or in GMCs, in order for the axons to make the right axonal pathfinding decisions or that *fru* function in other cell types, such as glial cells, is also required for wild-type axonal pathfinding. This explanation is supported by the finding of genetic interactions between *fru* and other genes involved in generating or responding to repulsive signaling of axons crossing the midline (H.-J. Song and B. J. Taylor, unpublished observations). Somewhat surprising was the finding that *fru* mutant embryos developed a more severe axonal defasciculation when *fru* transgenes were expressed only in neurons. The exacerbation of the *fru* mutant phenotype may indicate that the level of *fru* transcripts in neurons is important and that levels of Fru proteins different from those found in wild-type neurons might result in disruptions of normal axonal pathfinding or the interaction of these neurons with fru^- glial cells.

***fru*'s role in the embryonic CNS appears to be largely in the regulation of axonal outgrowth, not in the initial acquisition of neuronal identity:** The FasII and BP102 axonal pathfinding defects we found in *fru* mutant CNSs might result from the failure of neurons to adopt their proper cell fate or their ability to differentiate according to their fate. Since P3 and P4 *fru* transcripts are strongly expressed during NB delamination and early neurogenesis, the time at which neuronal fate decisions are being made, it was possible that *fru*'s main function would be in fate determination. We found that four neurons, dMP2, vMP2, aCC, and pCC, responsible for pioneering the medial and intermediate FasII tracts expressed the appropriate identity markers, Odd-skipped and FasII (Grenningloh *et al.* 1991; Spana and Doe

1996; Hidalgo and Brand 1997; Hidalgo and Booth 2000). These results suggest that in *fru* mutants these neurons have adopted, at least partially, their initial wild-type fate. In support of this finding, we found that in *fru* mutants lacking all or most *fru* transcripts, all aCC and pCC neurons express Even-skipped. The loss of *fru* function, however, does affect the ability of some of these neurons to maintain Even-skipped expression at later embryonic stages (H.-J. Song and B. J. Taylor, unpublished observations). We have not examined all possible markers for these neurons and it may be that some cell fate markers are not expressed appropriately in *fru* mutants. The delay in the onset of Hb expression in neuroblasts may also indicate that *fru* has a small early role in neurogenesis. In addition, we examined neuronal identity in a very small population of neurons that have a very specific pioneering function; it may very well be that the *fru* gene plays a role in establishing neuronal identity in other embryonic neurons.

In *fru* mutants, the earliest defects we observed in FasII pioneering neurons were in the orientation and outgrowth of their initial axonal projections. In some neurons, axonogenesis appeared to be delayed, whereas in other neurons the initial axonal process was oriented abnormally and/or did not appear to be fasciculating properly with other axons. If these pioneering axons are unable to form normal fascicles or are unable to coalesce into discrete fascicles, then other later developing neurons may also be expected to have difficulties in fasciculating along their normal pathways. These results suggest that the loss of *fru* function may very well affect the expression of the specific receptor systems on axons that are necessary to recognize their fasciculation partners (for review, see Goodman and Doe 1993; Goodman 1996; Tear 1999; Rusch and Van Vactor 2000). In the dMP2 and vMP2 neurons, the expression of the Futsch protein was also delayed, suggesting that this gene is a target of *fru* function (Hummel *et al.* 2000). Similar weak labeling of neurons by mab22C10 has also been described in embryos mutant for the *argos*, *pointed*, and *prospero* genes; these genes are known to be important for establishing cell fate and in some cases are required for the formation of FasII axonal tracts (E. Spana and N. Perrimon, personal communication; Freeman *et al.* 1992; Klämbt 1993; Spana and Doe 1995). There is no direct evidence that the loss of *futsch* expression in *fru* mutants leads to abnormalities or delays in the outgrowth of dMP2/vMP2 axons. The *UAS-fruA* and *UAS-fruC* transgenes were able to rescue the FasII axonal pattern without rescuing the initial defects in mab22C10 expression in dMP2/vMP2. Thus, it is possible that the defects in axonal outgrowth growth by these neurons depend on alterations in other proteins involved in axonogenesis or axonal pathfinding.

Glial cells have been implicated as important regulators of axonal pathfinding by neurons. Glial cells in the CNS can be grouped into two major categories, midline and the lateral glia, according to their position and gene expression profiles in wild-type embryos. Four segmental midline glial cells, closely associated with the developing commissures, are characterized by the expression of the epidermal growth factor receptor, *argos*, and *pointedP2* (Klämbt 1993; Giesen *et al.* 1997; for reviews, see Granderath and Klämbt 1999 and Jacobs 2000). Lateral glial cells consist of several functional subgroups and express the *pointedP1*, *repo*, and *glial cell missing* genes (Klämbt 1993; Campbell *et al.* 1994; Xiong *et al.* 1994; Halter *et al.* 1995; Hosoya *et al.* 1995; Jones *et al.* 1995). Lateral glial cells, identified by their expression of Repo, express Fru proteins. Cell counts in *fru* mutant embryos revealed no change in the number of Repo-immunoreactive glial cells in these embryos compared with wild type. Likewise, we could find no defects in the number of midline glial cells in *fru* mutant embryos.

Glial cells of both subtypes are required for the formation of the axonal scaffold of the ventral nerve cord (Giesen *et al.* 1997; Scholz *et al.* 1997; Granderath and Klämbt 1999; Hummel *et al.* 1999). The loss of lateral glial cells has been implicated in defasciculation phenotypes of *tramtrack* and *glial cells missing* mutant embryos (Jones *et al.* 1995; Giesen *et al.* 1997). Defasciculation of FasII axons has also been found in *repo* mutants in which lateral glial cells are largely present, but are in some way unable to support axonal fasciculation (Halter *et al.* 1995; Hidalgo and Booth 2000). Other studies have identified mutations in genes involved in midline or glial development causing defects in FasII and BP102 CNS tracts similar to the phenotypes of *fru* mutants (Klämbt 1993; Giniger *et al.* 1994; Spana and Doe 1995; Giesen *et al.* 1997; Scholz *et al.* 1997; Thomas 1998; Hummel *et al.* 1999). The phenotypic similarity between these mutants and *fru* raises the possibility that *fru* acts in the same pathway as these other genes in glial cells.

From our findings, we conclude that the *fru* gene functions in the process of axonal pathfinding by neurons in the embryonic CNS. The earliest neuronal defect that we observed was in the initial outgrowth of axons, which suggests that the *fru* gene plays an important role in neurons during axonogenesis. Since *fru* is expressed in neuronal progenitors as well as in neurons and glia, *fru* may also have a role in cell fate acquisition or maintenance in these cell types.

On the possible function of sex-nonspecific *fru* transcripts in the adult CNS: The male-specific Fru proteins derived from the male P1 transcripts are involved in the control of male-specific behaviors (Goodwin *et al.* 2000; Lee *et al.* 2000; Usui-Aoki *et al.* 2000; Lee and Hall 2001; Lee *et al.* 2001). *fru* transcripts from the P2, P3, and P4 promoters are also widely expressed in the CNS and other tissues in the developing males and females, as determined by *in situ* hybridization with anti-BTB and anti-Com riboprobes (Ryner *et al.* 1996; M. Foss and B. J. Taylor, personal communication). It seems likely

that these *fru* transcripts might also have the same function in the developing adult CNS as in the embryonic CNS. During metamorphosis, another period of extensive axonogenesis occurs to create the new neuronal circuits needed for adult-specific behaviors. By analogy with the embryonic phase of neuronal differentiation, we anticipate that Fru proteins generated from P2, P3, and/or P4 promoters will be required for the formation of wild-type axonal tracts in the adult CNS.

We thank N. Patel, A. Travers, and J. Skeath for generously supplying us with antibodies and J. C. Hall for critical advice and review. We also thank G. Carney, M. Foss, K. Latham, C. Rivin, T. Dreher, J. Giebultowicz, S. Tornquist, and anonymous reviewers for helpful comments on this work and manuscript. This work was supported by National Institutes of Health grant NS-33352 to B.S.B., J.C.H., and B.J.T. Current financial support to S.F.G., from the Wellcome Trust and Division of Molecular Genetics, University of Glasgow, is gratefully acknowledged. J.-C.B. is supported by a University of Glasgow postgraduate scholarship and an Overseas Research Studentship award.

LITERATURE CITED

Anand, A., A. Villella, L. C. Ryner, T. Carlo, S. F. Goodwin *et al.*, 2001 Molecular genetic dissection of the sex-specific and vital functions of the *Drosophila melanogaster* sex determination gene *fruitless*. Genetics **158:** 1569–1595.

Bainbridge, S. P., and M. Bownes, 1981 Staging the metamorphosis of *Drosophila melanogaster*. J. Embryol. Exp. Morphol. **66:** 57–80.

Bayer, C. A., L. von Kalm and J. W. Fristrom, 1997 Relationships between protein isoforms and genetic functions demonstrate functional redundancy at the *Broad-Complex* during *Drosophila* metamorphosis. Dev. Biol. **187:** 267–282.

Brand, A. H., and N. Perrimon, 1993 Targeted gene expression as a means of altering cell fate and generating dominant phenotypes. Development **118:** 401–415.

Broadus, J., and C. Q. Doe, 1995 Evolution of neuroblast identity: *seven-up* and *prospero* expression reveal homologous and divergent neuroblast fates in *Drosophila* and *Schistocerca*. Development **121:** 3989–3996.

Broadus, J., J. B. Skeath, E. P. Spana, T. Bossing, G. Technau *et al.*, 1995 New neuroblast markers and the origin of the aCC/pCC neurons in the Drosophila central nervous system. Mech. Dev. **53:** 393–402.

Brose, K., and M. Tessier-Lavigne, 2000 Slit proteins: key regulators of axon guidance, axonal branching, and cell migration. Curr. Opin. Neurobiol. **10:** 95–102.

Campbell, G., H. Göring, T. Lin, E. Spana, S. Andersson *et al.*, 1994 RK2, a glial-specific homeodomain protein required for embryonic nerve cord condensation and viability in *Drosophila*. Development **120:** 2957–2966.

Campos-Ortega, J. A., and V. Hartenstein, 1997 *The Embryonic Development of Drosophila melanogaster*. Ed. 2. Springer-Verlag, New York.

Castrillon, D. H., P. Gonzy, S. Alexander, R. Rawson, C. G. Eberhart *et al.*, 1993 Toward a molecular genetic analysis of spermatogenesis in *Drosophila melanogaster*: characterization of male-sterile mutants generated by single *P*-element mutagenesis. Genetics **135:** 489–505.

DiBello, P. R., D. A. Withers, C. A. Bayer, J. W. Fristrom and G. M. Guild, 1991 The Drosophila *Broad-Complex* encodes a family of related proteins containing zinc fingers. Genetics **129:** 385–397.

FlyBase, 1999 The FlyBase database of the Drosophila genome projects and community literature. Nucleic Acids Res. **27:** 85–88 (http://flybase.bio.indiana.edu/).

Freeman, M., C. Klämbt, C. S. Goodman and G. M. Rubin, 1992 The *argos* gene encodes a diffusible factor that regulates cell fate decision in the Drosophila eye. Cell **69:** 963–975.

Fujita, S. C., S. L. Zipursky, S. Benzer, A. Ferrus and S. W. Shotwell, 1982 Monoclonal antibodies against the Drosophila nervous system. Proc. Natl. Acad. Sci. USA **79:** 7929–7933.

Giesen, K., T. Hummel, A. Stollewerk, S. Harrison, A. Travers *et al.*, 1997 Glial development in the Drosophila CNS requires concomitant activation of glial and repression of neuronal differentiation genes. Development **124:** 2307–2316.

Giniger, E., K. Tietje, L. Y. Jan and Y. N. Jan, 1994 *lola* encodes a putative transcription factor required for axon growth and guidance in *Drosophila*. Development **120:** 1385–1398.

Goodman, C. S., 1996 Mechanisms and molecules that control growth cone guidance. Annu. Rev. Neurosci. **19:** 341–377.

Goodman, C. S., and C. Q. Doe, 1993 Embryonic development of the Drosophila central nerve system, pp. 1131–1206 in *Development of Drosophila melanogaster*, edited by M. Bate and A. Martinez-Arias. Cold Spring Harbor Laboratory Press, Cold Spring Harbor, NY.

Goodwin, S. F., B. J. Taylor, A. Villella, M. Foss, L. C. Ryner *et al.*, 2000 Aberrant splicing and altered spatial expression patterns in *fruitless* mutants of *Drosophila melanogaster*. Genetics **154:** 725–745.

Granderath, S., and C. Klämbt, 1999 Glia development in the embryonic CNS of Drosophila. Curr. Opin. Neurobiol. **9:** 531–536.

Grenningloh, G., E. J. Rehm and C. S. Goodman, 1991 Genetic analysis of growth cone guidance in Drosophila: *fasciclin II* functions as a neuronal recognition molecule. Cell **67:** 45–57.

Guthrie, S., 1999 Axon guidance: starting and stopping with slit. Curr. Biol. **9:** R432–R435.

Halter, D. A., J. Urban, C. Rickert, S. S. Ner, K. Ito *et al.*, 1995 The homeobox gene *repo* is required for the differentiation and maintaince of glia function in the embryonic nervous system of *Drosophila melanogaster*. Development **121:** 317–332.

Heinrichs, V., L. C. Ryner and B. S. Baker, 1998 Regulation of sex-specific selection of *fruitless* 5′ splice sites by transformer and transformer-2. Mol. Cell. Biol. **18:** 450–458.

Hidalgo, A., and G. E. Booth, 2000 Glia dictate pioneer axon trajectories in the Drosophila embryonic CNS. Development **127:** 393–402.

Hidalgo, A., and A. H. Brand, 1997 Targeted neuronal ablation: the role of pioneer neurons in guidance and fasciculation in the CNS of *Drosophila*. Development **124:** 3253–3262.

Hosoya, T., K. Takizawa, K. Nitta and Y. Hotta, 1995 *glial cells missing*: a binary switch between neuronal and glial determination in Drosophila. Cell **82:** 1025–1036.

Hummel, T., K. Schimmelpfeng and C. Klämbt, 1999 Commissure formation in the embryonic CNS of Drosophila. II. Function of the different midline cells. Development **126:** 771–779.

Hummel, T., K. Krukkert, J. Roos, G. Davis and C. Klämbt, 2000 Drosophila *futsch*/22C10 is a MAP1B-like protein required for dendritic and axonal development. Neuron **26:** 357–370.

Ito, H., K. Fujitani, K. Usui, K. Shimizu-Nishikawa, S. Tanaka *et al.*, 1996 Sexual orientation in Drosophila is altered by the *satori* mutation in the sex determination gene *fruitless* that encodes a Zinc finger protein with a BTB domain. Proc. Natl. Acad. Sci. USA **93:** 9687–9692.

Jacobs, J. R., 2000 The midline glia of Drosophila: a molecular genetic model for the developmental function of glia. Prog. Neurobiol. **62:** 475–508.

Jones, B. W., R. J. Fetter, G. Tear and C. S. Goodman, 1995 *glial cells missing*: a genetic switch that controls glial versus neuronal fate. Cell **82:** 1013–1023.

Klaes, A., T. Menne, A. Stollewerk, H. Scholz and C. Klämbt, 1994 The Ets transcription factors encoded by the Drosophila gene *pointed* direct glial cell differentiation in the embryonic CNS. Cell **78:** 149–160.

Klämbt, C., 1993 The Drosophila gene *pointed* encodes two ETS-like proteins, which are involved in the development of the midline glial cells. Development **117:** 163–176.

Krueger, N. X., D. Van Vactor, H. I. Wan, W. M. Gelbart, C. S. Goodman *et al.*, 1996 The transmembrane tyrosine phosphatase DLAR controls motor axon guidance in Drosophila. Cell **84:** 611–622.

Lee, G., and J. C. Hall, 2001 Abnormalities of male-specific FRU protein and serotonin expression in the central nervous system of *fruitless* mutants in Drosophila. J. Neurosci. **21:** 513–526.

Lee, G., M. Foss, S. F. Goodwin, T. Carlo, B. J. Taylor *et al.*, 2000

Spatial, temporal, and sexually dimorphic expression patterns of the *fruitless* gene in the *Drosophila* central nervous system. J. Neurobiol. **43:** 404–426.

Lee, G., A. Villella, B. J. Taylor and J. C. Hall, 2001 New reproductive anomalies in *fruitless*-mutant *Drosophila* males: extreme lengthening of mating durations and infertility correlated with defective serotonergic innervation of reproductive organs. J. Neurobiol. **47:** 121–149.

Lin, D. M., and C. S. Goodman, 1994 Ectopic and increased expression of Fasciclin II alters motoneuron growth cone guidance. Neuron **13:** 507–523.

Lin, D. M., R. D. Fetter, C. Kopczynski, G. Grenningloh and C. S. Goodman, 1994 Genetic analysis of Fasciclin II in Drosophila: defasciculation, refasciculation, and altered fasciculation. Neuron **13:** 1055–1069.

O'Neill, E. M., I. Rebay, R. Tijan and G. M. Rubin, 1994 The activities of two Ets-related transcription factors requred for Drosophila eye development are modulated by the Ras/MAPK pathway. Cell **78:** 137–147.

Patel, N. H., 1994 Imaging neuronal subsets and other cell types in whole-mount Drosophila embryos and larvae using antibody probes, pp. 445–487 in *Drosophila melanogaster*: *Practical Uses in Cell and Molecular Biology*, edited by L. S. B. Goldstein and E. A. Fryberg. Academic Press, San Diego.

Patel, N. H., E. Martin-Blanco, K. G. Coleman, S. J. Poole, M. C. Ellis *et al.*, 1989 Expression of *engrailed* proteins in arthropods, annelids, and chordates. Cell **58:** 955–968.

Restifo, L. L., and W. Hauglum, 1998 Parallel molecular genetic pathways operate during CNS metamorphosis in Drosophila. Mol. Cell. Neurosci. **11:** 134–148.

Restifo, L. L., and V. K. Merrill, 1994 Two Drosophila regulatory genes, *deformed* and the *Broad-Complex*, share common functions in development of adult CNS, head, and salivary glands. Dev. Biol. **162:** 465–485.

Robertson, H. M., C. R. Preston, R. W. Phillis, D. M. Johnson-Schlitz, W. K. Benz *et al.*, 1988 A stable genomic source of P element transposase in *Drosophila melanogaster*. Genetics **118:** 461–470.

Rubin, G. M., and A. C. Spradling, 1982 Genetic transformation of Drosophila with transposable element vectors. Science **218:** 348–353.

Rusch, J., and D. Van Vactor, 2000 New Roundabouts send axons into the Fas lane. Neuron **28:** 637–640.

Ryner, L. C., S. F. Goodwin, D. H. Castrillon, A. Anand, A. Villella *et al.*, 1996 Control of male sexual behavior and sexual orientation in Drosophila by the *fruitless* gene. Cell **87:** 1079–1089.

Sandstrom, D. J., C. A. Bayer, J. W. Fristrom and L. L. Restifo, 1997 *Broad-Complex* transcription factors regulate muscle attachment in Drosophila. Dev. Biol. **181:** 168–185.

Scholz, H., E. Sadlowski, A. Klaes and C. Klämbt, 1997 Control of midline glia development in the embryonic Drosophila CNS. Mech. Dev. **64:** 137–151.

Seeger, M., G. Tear, D. Ferres-Marco and C. S. Goodman, 1993 Mutations affecting growth cone guidance in Drosophila: genes necessary for guidance towards or away from the midline. Neuron **10:** 409–426.

Smith, D. B., 1993 Purification of glutathione-S-transferase fusion proteins. Methods Mol. Cell. Biol. **4:** 220–229.

Spana, E. P., and C. Q. Doe, 1995 The prospero transcription factor is asymmetrically localized to the cell cortex during neuroblast mitosis in *Drosophila*. Development **121:** 3187–3195.

Spana, E. P., and C. Q. Doe, 1996 Numb antagonizes Notch signaling to specify sibling neuron cell fates. Neuron **17:** 21–26.

Spana, E. P., C. Kopczynski, C. S. Goodman and C. Q. Doe, 1995 Asymmetric localization of numb autonomously determines sibling neuron identity in the Drosophila CNS. Development **121:** 3489–3494.

Spradling, A. C., D. Stern, A. Beaton, E. J. Rhem, T. Laverty *et al.*, 1999 The Berkeley *Drosophila* Genome Project gene disruption project: single *P*-element insertions mutating 25% of vital Drosophila genes. Genetics **153:** 135–177.

Sun, Q., S. Bahri, A. Schmid, W. Chia and K. Zinn, 2000 Receptor tyrosine phosphatases regulate axon guidance across the midline of the Drosophila embryo. Development **127:** 801–812.

Tear, G., 1999 Neuronal guidance. A genetic perspective. Trends Genet. **15:** 113–118.

Thomas, J. B., 1998 Axon guidance: crossing the midline. Curr. Biol. **8:** R102–R104.

Usui-Aoki, K., H. Ito, K. Ui-Tei, K. Takahashi, T. Lukacsovich *et al.*, 2000 Formation of the male-specific muscle in female Drosophila by ectopic *fruitless* expression. Nat. Cell Biol. **2:** 500–506.

van Roessel, P., and A. H. Brand, 2000 GAL4-mediated ectopic gene expression in Drosophila, pp 439–447 in *Drosophila Protocols*, edited by W. Sullivan, M. Ashburner and R. S. Hawley. Cold Spring Harbor Laboratory Press, Cold Spring Harbor, NY.

Villella, A., D. A. Gailey, B. Berwald, S. Ohshima, P. T. Barnes *et al.*, 1997 Extended reproductive roles of the *fruitless* gene in *Drosophila melanogaster* revealed by behavioral analysis of new *fru* mutants. Genetics **147:** 1107–1130.

Xiong, W.-C., H. Okano, N. H. Patel, J. A. Blendy and C. Montell, 1994 *repo* encodes a glial-specific homeodomain protein required in the Drosophila nervous system. Genes Dev. **8:** 981–994.

Yeo, S. L., A. Lloyd, K. Kozak, A. Dinh, T. Dick *et al.*, 1995 On the functional overlap between two Drosophila POU homeodomain genes and the cell fate specification of a CNS neural precursor. Genes Dev. **9:** 1223–1236.

Zollman, S., D. Godt, G. G. Prive, J. L. Couderc and F. A. Laski, 1994 The BTB domain, found primarily in zinc finger proteins, defines an evolutionarily conserved family that includes several developmentally regulated genes in Drosophila. Proc. Natl. Acad. Sci. USA **91:** 10717–10721.

Communicating editor: T. Schüpbach